STREEM™ – InGaN Edition

STRain Engineering in Electronic Materials

User Guide

November 2015

User Support: STREEM-Support@str-soft.com
Software Sales: STR-sales@str-soft.com
Phone: +7 812 320 4390 Fax: +7 812 326 6194
STR Group Inc. www.str-soft.com
Engels av. 27, P.O. Box 89, 194156, St. Petersburg, Russia

Table of Contents

1. Introduction

Nowadays, III-nitride electronic and optical devices (LEDs, laser diodes, transistors, etc.) are actively developed in order to achieve higher performance at lower cost that would expand their areas of applications. Aside from the device design, much effort is focused on tuning and refining the conditions and recipes used to grow epitaxial structures with desired properties. Optimization of the growth conditions and choice of the best epitaxy procedure providing high quality materials with targeted composition and doping is rather nontrivial, especially in the case of III-nitride semiconductors. Varying such parameters as the reactor pressure, carrier gas composition, precursor flow rates, and growth temperature, as well as the use of special procedures like growth interruptions, pre-depositions, and temperature ramping is known to impact strongly the performance of nominally the same device structures. Depending on particular recipe and structure design, modifications of the growth conditions may induce changes in compositional and structural properties of the grown crystals, affecting distributions of strain and defect density in the grown heterostructures. In turn, this may lead to dramatic changes in optical and electrical device characteristics. Detailed understanding and quantification of correlations between the growth recipe and heterostructure properties is a key factor providing successful optimization of epitaxial technology.

STREEM-InGaN is a specialized software tool for modeling the characteristics of (0001) III-Nitride device heterostructures grown by MOCVD from conventional metal-organic precursors (TMIn, TMGa/TEGa, TMAl) and ammonia, diluted in H_2/N_2 carrier gases. STREEM-InGaN focuses on an InGaN-based active region which implies a sequence of quantum wells and barriers as well as other stages in-between. Layers grown prior to and after the active region can be added into the simulations as well.

The software is aimed at understanding and control of the structure properties by adjusting the process recipe. In particular, the following issues can be addressed:

- influence of the process parameters on indium incorporation into the quantum wells;
- predictions of the actual composition profile in the active region of the heterostructure, including delayed indium incorporation into the QWs and indium tails in the cap layers or barriers. Due to indium surface segregation, the actual composition profile normally deviates from the nominal one built up from the steady-state solutions obtained for every individual epilayer at the respective growth conditions;
- consistent computations of indium incorporation and elastic energy allows the users to follow and adjust the strain distribution in the active region by both modifying the operating parameters for the

particular layers and adding strain-relief layers underneath the quantum wells. The actual composition and strain profiles determine the distribution of the polarization charges in the structure that can be accounted for in subsequent modeling of device operation with the SiLENSe software [http://www.str-soft.com/products/SiLENSe/];

- stress relaxation via formation of V-shaped dislocation half-loops, annihilation of the threading dislocations, and evolution of the strain, threading dislocation density, and indium composition profile can be studied with the STREEM-InGaN software, depending on the particular parameters in the recipe.

As a result of the modeling, the user can analyze such characteristics as the growth rate and composition profile across the heterostructure and the distributions of strain and dislocation density. By adjusting the recipe parameters, including temperature, pressure, flow rates of the precursors and carrier gases, as well as the sequence and durations of the particular stages of the process, the user can follow the respective changes in the above characteristics and establish correlations between the recipe and properties of the heterostructure.

The user is welcome to contact STR by e-mail STREEM-Support@str-soft.com with any problems or questions about STREEM operation.

2. Installation and licensing

2.1 Installation

To install the STREEM-InGaN software, run the installation executable file and follow the installer instructions. To uninstall the program, run the ***unins000.exe*** file in the program home directory or use the respective item in the *Programs* menu. Note that the software needs write permission for its home directory.

After the installation, the STREEM-InGaN package includes the following items:

- ***STREEM-InGaN.exe*** executable file and dll files required for software operation;
- ***Doc*** folder that contains the User Guide;
- ***Examples*** folder that contains a number of example cases;
- Files required for licensing the software

The software is supplied with the license protection system based on a dongle key which is a small USB device. During installation, the user is prompted to install the dongle key driver.

2.2 Single node license

The user can install the program on several PCs (for example, on the desktop and notebook) and run the program on the PC where the dongle key is plugged in. The registration procedure is as follows:

- Plug in the dongle key module;
- Start the license manager (License.exe) located the STREEM-InGaN home directory. One can also do it by Windows Start button;
- Choose the *Key config* tab and press the *Make Key* button. The request file (****.req***) containing the information about the dongle will be generated;
- Send the generated request file to STR by e-mail STREEM-support@str-soft.com;
- When the reply from STR is received, plug in the dongle, start the license manager, press *Accept Key* button, and browse for the license file (****.lic***) received from STR;
- Now one can run STREEM-InGaN.

Note that the maximum number of simultaneous runs of the software is limited as specified in the particular license agreement (quotation, purchase order, etc.).

2.3 Corporate/department network license

Corporate/department license allows the user to run the software on several computers within the local area network (LAN). The software may be installed on any computer of the network, but the maximum number of simultaneously running copies of the software is limited as specified in the particular license agreement (quotation, purchase order, etc.).

Hereafter, by the ‘server’ we will understand the computer where the USB dongle key is plugged in. The user should install the dongle key driver on this PC. A special tool ***server.exe*** called below ‘license server’ to be running on the server computer. After start, the respective icon appears in the system tray. The pop-up menu allows one to restore the window and inspect the event log or the license server. The *Change Port* button allows the user choose the port number for communication between the software running on other PCs and the license server.

To obtain/update the license, one needs to run the ***License.exe*** file on the server PC. Further procedure is similar to that described in Section 2.2.

All the PCs running the STREEM-InGaN software we will call ‘workstations’. Running the software on the server computer is also allowed. Installation of the software on the workstations is described in Section 2.1. The user does not need to install the dongle key driver on workstations. Instead, one should run the ***License.exe*** file, choose *Server config* tab, and specify the IP address of the server PC and the port number. The *Store* button saves this information in the ***Str_Config_SL.cfg*** file in the software home directory. This file is used by the software to communicate with the license server. The *Remove* button clears the file. The *Test* button allows one to test the communication with the license server. The following conditions to be fulfilled for running the software on a certain workstation: (i) the dongle key to be plugged into the server PC, (ii) license server to be running on the server PC, and (iii) the workstation is able to communicate with the license server by the IP address and port number specified in the ***Str_Config_SL.cfg*** file in the software home directory. Unplugging the dongle key from the server PC or stopping the license server will result in abnormal termination of all the running software copies.

3. Theoretical background

3.1 Governing equations to describe composition profile in device heterostructures

The underlying surface kinetic model considers MOCVD of several $In_xGa_yAl_{1-x-y}N$ layers of arbitrary composition. The growth is assumed to occur from typical MO compounds, namely, TMIn, TMGa/TEGa, and TMAl as the group-III precursors and NH_3 as the N precursor. Pure N_2 or possibly a mixture of N_2 and H_2 are used as the carrier gas. The structure is grown via diffusion of the precursors through the concentration boundary layer that is formed above the growth surface and determined by the gas species transport in particular MOCVD reactors. The incoming gas species decompose at the growth surface to produced adsorbed atoms of In, Ga, Al, N, and H, which partly desorb back to the gas in the form of the initial gas species and monatomic In, Ga, and Al and partly incorporate into the crystal to produce solid solution $In_xGa_yAl_{1-x-y}N$.

The model utilizes an approach that was suggested and then developed in Refs. [1-3]. The approach is based on the unsteady balance of the adsorbed species and is described by the kinetic equations as follows.

$$\frac{d\theta_{In}}{dt} = \sum_g J_g \nu_{g,In} - J_{InN} \tag{1}$$

$$\frac{d\theta_{Ga}}{dt} = \sum_g J_g \nu_{g,Ga} - J_{GaN} \tag{2}$$

$$\frac{d\theta_{Al}}{dt} = \sum_g J_g \nu_{g,Al} - J_{AlN} \tag{3}$$

$$\frac{d\theta_{N}}{dt} = \sum_g J_g \nu_{g,N} - J_{InN} - J_{GaN} - J_{AlN} \tag{4}$$

$$\frac{d\theta_{H}}{dt} = \sum_g J_g \nu_{g,H} \tag{5}$$

$$\frac{X}{Y} = \frac{J_{InN}}{J_{GaN}} \tag{6}$$

$$\frac{X}{1-X-Y} = \frac{J_{InN}}{J_{AlN}} \tag{7}$$

Here, θ_a are the surface molar densities of the adsorbed atoms (*a* = In, Ga, Al, N, and H), J_g are the gas species molar fluxes between the gas and adsorbed layer (*g* = TMIn, TMGa/TEGa, TMAl, NH_3, N_2, H_2, In, Ga, and Al), $\nu_{g,a}$ are the stoichiometric coefficients, J_{InN}, J_{GaN}, and J_{AlN} are the corresponding molar fluxes between the adsorbed layer and the crystal, and X and Y are respectively the InN and GaN molar fractions in $In_xGa_yAl_{1-x-y}N$.

The gas-adsorbate fluxes are found as

$$J_g = \frac{P_g^0 - K_g \prod_a (\theta_a)^{\nu_{g,a}}}{R_g} \tag{8}$$

where P_g^0 are the species partial pressures at the conventional external border of the concentration boundary layer (i.e. at the interface between the boundary layer and the flow core), K_g are the reduced desorption rate constants, and R_g are the transport resistances between the flow concentration core and the growth surface.

Species partial pressures can be found as $P_g^0 = PG_g / G$, where P is the total pressure, G_g are the species input molar fluxes, and $G = \sum_g G_g$ is the total input molar flux. The species transport resistances are given as

$$R_g = R_g^d + R_g^k \tag{9}$$

where $R_g^d = RT\delta / D_g$ are the diffusion resistances, $R_g^k = 1/\alpha_g\beta_g$ are the kinetic (Knudsen) resistances, D_g are the diffusivities, R is the gas constant, T is the temperature, δ is the concentration boundary layer thickness, α_g are the sticking coefficients, $\beta_g = (2\pi m_g RT)^{1/2}$ are the Hertz-Knudsen factors, and m_g are the molar masses.

The adsorbate-solid fluxes are found as

$$J_{InN} = K_{InN}^+ \theta_{In}\theta_N - K_{InN}^- \gamma_{InN}\chi_V X \ , \ J_{GaN} = K_{GaN}^+ \theta_{Ga}\theta_N - K_{GaN}^- \gamma_{GaN}\chi_V Y \ ,$$
$$J_{AlN} = K_{AlN}^+ \theta_{Al}\theta_N - K_{AlN}^- \gamma_{AlN}\chi_V (1 - X - Y) \tag{10}$$

where K_i^+ (*i* = InN, GaN, AlN) are the rate constants of the constituents incorporation into the solid

solution $In_xGa_yAl_{1-x-y}N$, K_i^- are the rate constants of the constituents going out from the solid solution, γ_i, are the constituents activities, and χ_V is the surface coverage with vacancies. Quantities γ_i determine deviation of $In_xGa_yAl_{1-x-y}N$ from the ideal solution model and are related to two factors: energies of interaction of the constituents in the solid solution and distribution of stress in the structure. The $In_xGa_yAl_{1-x-y}N$ growth rate is eventually determined as

$$V_{gr} = J_{InN}W_{InN} + J_{GaN}W_{GaN} + J_{AlN}W_{AlN} \quad (11)$$

where W_{InN}, W_{GaN}, and W_{AlN} are the corresponding molar volumes.

Due to the detailed balance principle, kinetic constants are not totally independent but related to each other by the conditions of equilibrium, corresponding to four overall surface reactions

$NH_3(g) <=> (1/2)N_2(g) + (3/2)H_2(g)$ (R1)

$In(g) + (1/2)N_2(g) <=> InN(s)$ (R2)

$Ga(g) + (1/2)N_2(g) <=> GaN(s)$ (R3)

$Al(g) + (1/2)N_2(g) <=> AlN(s)$ (R4)

Analysis of numerous literature data suggests that formation of the composition profile in the considered heterostructures is largely limited by the desorption of atomic In from the growth surface and thus is determined by the In desorption rate constant that is approximated as a function of temperature, $K_{In}(T)$. Sticking probability of low-reactive N_2 is approximated as a function of temperature and solid solution composition, $\alpha_{N2}(T, X, Y)$, while those of the other species, except for the In-containing species, are assumed unity. Sticking probabilities of the In-containing species depend on the capacity of In adsorbed layer. Two models of the In adsorbed layer are incorporated into the software, one limits its capacity to one monolayer while the other does not limit it at all. Thus, the two models correspond to the lower and upper limits of the In adsorbed layer capacity. In the former case, the sticking probabilities of the In-containing species are not unity due to site blocking with adsorbed indium and can be found as

$$\alpha_g = \chi_V = 1 - \theta_{In}/\theta_s \quad (12)$$

where θ_s is the surface molar density of the In adsorption sites.

Given the process recipe, i.e. the growth temperature, pressure, and the species flow rates as functions of time, $T(t)$, $P(t)$, and $G_g(t)$, the developed kinetic model represents a closed stiff set of seven differential-algebraic equations (1)-(7) with supplementary relationships (8)-(12) in seven unknown

functions of time, $\theta_a(t)$, $X(t)$, and $Y(t)$. The software solves it numerically using the Radau method with automatic adaptation of time steps, which is just aimed at the solution of stiff problems. With the derived solution, the gas-adsorbate fluxes, the adsorbate-crystal fluxes, and the growth rate are also found as functions of time, $J_g(t)$, $J_{InN}(t)$, $J_{GaN}(t)$, $J_{AlN}(t)$, and $V_{gr}(t)$. Then, the interface displacement relative to its initial position is found from equation

$$\frac{dz}{dt} = V_{gr} \tag{13}$$

Eventually, the desirable composition profiles in the structure, $X(z)$ and $Y(z)$, are implicitly determined by three functions of time, they are $X(t)$, $Y(t)$, and $z(t)$.

3.2 Contribution of stress and mixing energies to the InGaAlN growth chemistry

Stress and mixing energies affect incorporation of In, Ga, and Al into the structure via deviation of realistic $In_xGa_yAl_{1-x-y}N$ solid solution from the ideal solution model. The effect is associated with some change of the equilibrium constants of overall surface reactions (R2)-(R4) due to the change of chemical potentials of the solid solution constituents, i.e. InN, GaN, and AlN. Chemical potentials of the gas species little differ from those of ideal gases

$$\mu_g = \mu_g^0(T) + RT\ln(P_g / P_s) \tag{14}$$

where $\mu_g^0(T)$ are the temperature-dependent chemical potentials under the standard pressure P_s. Simultaneously, chemical potentials of the constituents essentially differ from those in the ideal solution due to the considerable energies of their interaction and additional elastic energy. Following the approach developed in Refs. [4,5], these potentials are found as

$$\begin{aligned}
\mu_{InN} &= W_{InGaN}Y^2 + W_{InAlN}(1-X-Y)^2 + (W_{InGaN} + W_{InAlN} - W_{GaAlN})Y(1-X-Y) + \mu_{InN}^s \\
\mu_{GaN} &= W_{InGaN}X^2 + W_{GaAlN}(1-X-Y)^2 + (W_{InGaN} + W_{GaAlN} - W_{InAlN})X(1-X-Y) + \mu_{GaN}^s \\
\mu_{AlN} &= W_{InAlN}X^2 + W_{GaAlN}Y^2 + (W_{InAlN} + W_{GaAlN} - W_{InGaN})XY + \mu_{AlN}^s
\end{aligned} \tag{15}$$

where W_{InGaN}, W_{InAlN}, and W_{GaAlN} are the energies of interaction of the corresponding binary constituents in $In_xGa_yAl_{1-x-y}N$ and μ_{InN}^s, μ_{GaN}^s, and μ_{AlN}^s are the contributions of elastic energy.

The latter quantities are determined by two factors: elastic strain arising due to the difference between

the crystal lattice constants at the growth surface and in the last underlying layer (i) and plastic strain induced by the initial threading dislocations and V-shaped dislocation half-loops (HLs), which may arise during the growth of heterostructure in the active region (ii). As it is shown in Ref. [6], formation of such dislocations represents the major mechanism of stress relaxation in compressed (0001)-directed heterostructures, consistent with the main experimental findings and providing reasonable agreement of calculated and experimental data on the critical thickness. Then the stress parts of chemical potentials are found as

$$\mu_i^s = \frac{\sqrt{3}}{4} c_s N_A B \Delta a^2 \left(\frac{B_i}{B} + 2\frac{\Delta a_i}{\Delta a} - 2 \right), \; i = \text{InN, GaN, AlN} \qquad (16)$$

Here, c_s is the lattice constant of the last underlying layer, N_A is Avogadro number, $\Delta a_i = a_i - a_s$, a_i are the effective lattice constants of the constituents accounting for the plastic strain, a_s is the lattice constant of the last underlying layer, B_i are the biaxial modulus of the constituents, and $B = B_{InN}X + B_{GaN}Y + B_{AlN}(1-X-Y)$ and $\Delta a = \Delta a_{InN}X + \Delta a_{GaN}Y + \Delta a_{AlN}(1-X-Y)$ are the corresponding averaged values.

Quantities μ_i^s eventually represent explicit functions of the lattice and elastic constants of the constituents (i) and parameters of the plastic strain, namely, surface density of threading dislocations, ρ_{TD}, angle of HL opening, α, and coordinate of HL apex, z_0 (ii). Angle α is considered as an input parameter of the problem while quantities ρ_{TD} and z_0 are found during solution of the problem.

Accounting for the fact that each dislocation HL has two wings and each of the wings represents a threading dislocation, the total threading dislocation density is found as

$$\rho_{TD} = \rho_{TD}^0 + 2\rho_{VD} \qquad (17)$$

with ρ_{TD}^0 being the user specified density of the threading dislocations in the layers underneath the active region and ρ_{VD} being the density of HLs. Then, two extensions of the model are introduced as compared to the first release:

- dislocations are sloped at angle α in the compressed regions of the heterostructure but become vertical in the regions with tensile stress, which can appear during the growth;
- the sloped dislocations annihilate as they approach to each other closer than certain critical distance, that is so called characteristic annihilation radius r_a.

With these two extensions, the desirable quantities ρ_{TD} and z_0 are found from the kinetic equation of dislocation annihilation (similarly to Ref. [7]) in combination with the energy balance similar to that used in Ref. [6] to derive the critical thickness for the generation of dislocations

$$\frac{d\rho_{TD}}{dz} = -2r_a\rho_{TD}^2 tg(\alpha) \quad (18)$$

$$\Delta E(z, z_0, \rho_{TD}) = E(z, z_0) - W(z, z_0, \rho_{TD}) = 0 \quad (19)$$

Here, $E(z, z_0)$ is the self-energy of the V-shaped dislocation HLs and $W(z, z_0, \rho_{TD})$ is the energy release of the biaxial mismatch stress to produce the dislocation HL.

Eqs. (1)-(7) are solved numerically jointly with supplementary relationships (8)-(16) and kinetic equation (18), with criterion (19) being controlled at every time step. Initially, as the interface coordinate z is not too high, there are no V-shaped dislocation HLs ($\rho_{VD} = 0$) and Eq. (19) is not satisfied at any z_0. However, at some (critical) coordinate z_c, criterion (19) becomes valid for some value of z_0. At this moment, the dislocations are generated with the apex located at z_0. Further, z_0 does not vary, while the dislocation density ρ_{TD} changes following kinetic equation (18) and continuously satisfying criterion (19).

4. Overview of the Graphical User Interface

Operation of the STREEM-InGaN software is implemented via Graphical User Interface (GUI) that is launched with the ***STREEM-InGaN.exe*** executable file. STREEM-InGaN GUI is aimed at working with the project files, specifying main computational parameters, defining process conditions, running computations, and viewing results. The STREEM-InGaN GUI contains the menu bar and a number of window tabs as follows 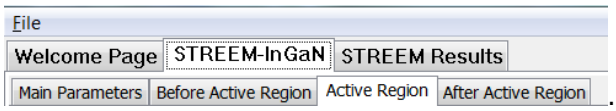

.

- *File* menu contains several conventional options to work with the project files, as described in Section 5;
- ***Welcome Page*** tab allows the users to create a new project, open any existing project, and open a project from the list of the recently open projects. More details are given in Section 5;
- ***STREEM-InGaN*** tab contains a number of items, namely:
    - ***Main Parameters*** tab to specify the governing parameters such as the surface segregation and stress relaxation models, units, and reactor transport model (see Section 6 for details);
    - ***Before Active Region***, ***Active Region***, and ***After Active Region*** tabs to specify the recipe for the corresponding stages of the process, as discussed in Section 7;
- ***STREEEM Results*** tab to visualize the modeling results, as discussed in Section 8.

To make the work with the STREEM-InGaN software more convenient, some features of the GUI can be adjusted by the user, depending on the particular settings of the computer (screen size and resolution, desktop font size, etc.). The font for the information specified in the recipe table can be changed by pressing 

button and subsequent selection of the desired items in the standard Windows dialog shown in Fig. 4.1.

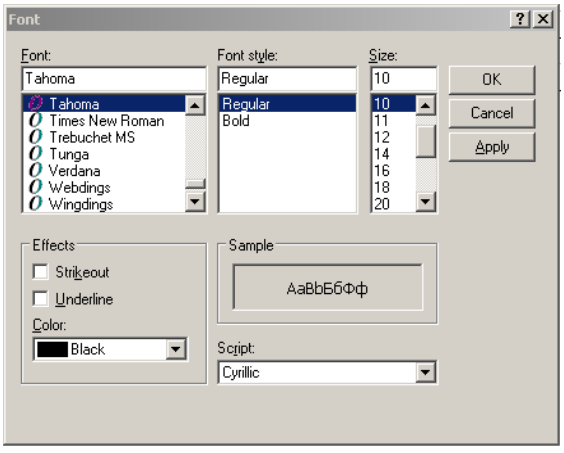

Fig. 4.1

Width of each particular column in the recipe table can be adjusted by dragging column border with the left mouse button. In case some information is beyond the screen, it can be approached with horizontal and vertical scrollbars. Other adjustable parameters are related to visualization of the results and discussed in Section 8.

Once adjusted, the above GUI settings will be used in all subsequent launchings of the GUI, until any changes are introduced.

5. Working with the project files and Welcome Page

Information specified by the user within the STREEM-InGaN GUI is stored in a ***project_name.stm*** file. Standard commands, including *New*, *Open*, *Save*, and *Save as*…, are available in the *File* menu bar of the GUI. Information stored in the ***project_name.stm*** file can be easily loaded into the STREEM-InGaN GUI by pressing the file, if the files with the ***stm*** extension are associated with the GUI during software installation.

Welcome Page is designed to provide quick access to the options of working with the project files. In particular, the user is allowed to open an existing project file with the *Open Project…* item on the left panel of the ***Welcome Page*** and start a new project with the *New Project…* item. In the latter case, the user is redirected to the ***Main Parameters*** tab of the GUI. On the ***Welcome Page*** it is also possible to load one of the recently opened projects from the respective list *Recently Opened Projects*; this list can be refreshed and non-existing files can be deleted from the list with the *Refresh* and *Delete Non Existing* items on the bottom panel of the ***Welcome Page***.

6. Specification of the main parameters

Before setting the growth recipe and making computations, the user is to specify some governing parameters on the ***Main Parameters*** tab of the GUI. These parameters include: selection of the surface segregation and stress relaxation models, choice of the units, and specification of the reactor transport model. Below, all these options are described in more detail.

6.1 Units

In this section, the user is to select, using the corresponding drop-down menu, the units for the temperature, pressure, growth rate, and group-III precursor flow rates. The selected units will be used throughout the project and can be changed on the ***Main Parameters*** tab only. Note that a change of a unit does not provide automatic re-calculation of the specified process parameters: e.g., if the pressure unit is changed from *Pa* to *mbar*, the operating pressure of 10,000 Pa will not automatically change to 100 mbar. The only exception is the growth rate for the layer outside the active region, as discussed in Section 7.3. The list of units allowed within the STREEM-InGaN is given in Table 6.1.

Process parameter	Units
Temperature	C, K
Pressure	Pa, Torr, mbar
Group-III flow rate	sccm, μmol/min
Growth rate	μm/h, nm/sec

Table 6.1

6.2 Segregation Model

As described in Section 3, there are two options related to the surface segregation models included into the STREEM-InGaN software, which consist in the account of or ignoring surface site blocking with adsorbed indium. The model can be selected via the corresponding radio button in the *Segregation Model* section on the ***Main Parameters*** tab. The nominal composition profile, corresponding to the absence of any segregation effects, can also be simulated by selecting *No segregation* option.

6.3 Relaxation Model

Stress relaxation in the InGaAlN/GaN active region via formation of V-shaped dislocation half-loops can be considered by clicking the corresponding radio button in the *Relaxation Model* section on the ***Main Parameters*** tab. Otherwise, the active region is assumed to grow pseudomorphically on the underlying

layer (by default, GaN is assumed, but other layer can be specified by the user, as discussed in Section 7.3).

6.4 Reactor Transport Model

As discussed in Section 3, mass transport is treated within the boundary layer concept. There are three options to specify the characteristics of mass transport in the reactor, the active option is chosen by clicking the corresponding radio button in the *Reactor Transport Model* section:

- *Fixed diffusion layer thickness*: when selecting this option, the user is to specify directly the boundary layer thickness (δ) for each stage in the active region;

- *Calibration on thick GaN growth rate*: as a rule, the growth rate of a thick GaN layer is well known for some particular process parameters. If it is the case, this information can be used for calibration purpose. When *Calibration on thick GaN growth rate* item is selected, an additional section *Reactor Model* and a table for specifying GaN process conditions appear. Since the boundary layer thickness is computed differently for different reactor types, the reactor type should be selected via the proper radio button in the *Reactor Model* section. Here, we distinguish three types of the reactor: close coupled showerhead, planetary/horizontal, and rotating disk.
  To set the reference GaN process conditions, the user is to fill the corresponding table. Here, the operating parameters are: temperature, pressure, carrier gas (N_2 and H_2) and ammonia flow rates, TMGa flow rate, and the reference growth rate. In case the rotating disk reactor, additional parameter, namely, the susceptor rotation rate (*rpm*) should be specified. Note that the TMGa flow rate (more general, group-III precursor flow rates for the active region) can be specified either directly or using bubbler characteristics, as described in Section 7.2.
  The reference GaN process parameters are used to estimate the boundary layer thickness at the stage of thick GaN growth (reference thickness). The latter quantity is then scaled at each stage of the heterostructure growth in the active region with the account for the corresponding differences in process conditions.

- *Calibration on average growth rate and composition*: selection of this option assumes that the user will have to specify an average growth rate and composition for each layer in the active region, so that the boundary layer thickness will be adjusted to get these values in the modeling. Presently, the software utilizes the partial GaN growth rate ($Vg^{GaN} \sim (1 - X_{In} - X_{Al}) \cdot Vg^{InGaAlN}$) to estimate the boundary layer thickness, so that the resulting layer composition may be somewhat different from the values specified by the user.

General view of the *Reactor Transport Model* section with specified process parameters for reference GaN is shown in Fig. 6.1.

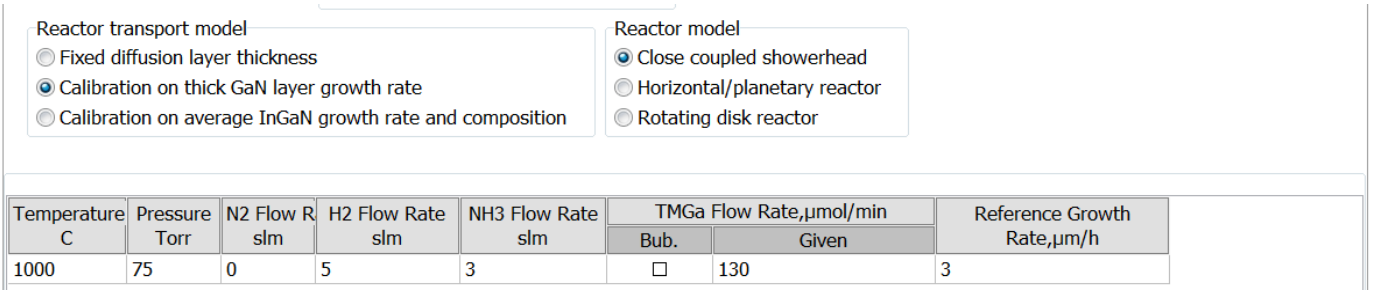

Temperature C	Pressure Torr	N2 Flow R slm	H2 Flow Rate slm	NH3 Flow Rate slm	TMGa Flow Rate,µmol/min		Reference Growth Rate,µm/h
					Bub.	Given	
1000	75	0	5	3	☐	130	3

Fig. 6.1

7. Specification of the recipe

Within the STREEM-InGaN software, the overall recipe is divided into three groups: stages (or layers) before the active region, active region, and stages after the active region. Parameters for these groups are specified on the respective tabs of the GUI.

To remind, an active region implies a sequence of quantum wells and barriers as well as other stages and special procedures in-between, like cap layer, pre-deposition, growth interruption, temperature ramping, etc. Modeling of the stress and composition profile is actually performed for the active region, so that it is important to specify correct process parameters for each stage of the active region. In case the recipe includes an underlayer or technological superlattice, it is recommended to include such layer in the active region to account for possible stress relaxation (see Example 4).

The recipe is represented as a table; depending on the layer position, each stage is described by one (for the layers outside the active region) or two lines (for the layers in the active region) in the table. The number of columns (actually, of the parameters to be specified) is also different for the layers within or outside the active region, as discussed below.

For each stage of the process, the first column in the table is the *Repeat Count* flag (indicates that the stage belongs to a group), the second one is the *Stage Number*, and the third one is the stage *Name* (can be optionally set by the user). Meaning of other parameters in the table is explained below. General view of the recipe table for the layers before/after the active region and inside the active region is shown in Fig. 7.1. The active line of the table is marked with dark blue; the active cell is marked with yellow. In case of a wrong value (e.g., negative flow rate) is specified, this cell is colored with red.

Welcome Page | STREEM-InGaN | STREEM Results

Main Parameters | Before Active Region | Active Region | After Active Region

Repeat Count	Stage Number	Name	Thickness characteristics						Composition						Dislocation density 1/cm²		Stress state			
			Thickness,nm		Duration,sec		Growth rate,μm/h		AlN		GaN		InN							
			Calc	Given	Calc	Given	Calc	Given	Calc	Given	Calc	Given	Calc	Given	Inherited	Given	Used	a,Å	Used	Relax.Degree
	1	n-GaN	○	450	◉	810	○	2	◉	0	○	1	○	0	□	1e10	◉	3.189	○	

Main Parameters | Before Active Region | Active Region | After Active Region

Repeat Count	Stage Number	Name	Thickness characteristics						Composition						Dislocation density 1/cm²		Stress State			
			Thickness,nm		Duration,sec		Growth rate,μm/h		AlN		GaN		InN							
			Calc	Given	Calc	Given	Calc	Given	Calc	Given	Calc	Given	Calc	Given	Inherited	Given	Used	a,Å	Used	Relax.Degree
	1	AlGaN	○	30	◉	540	○	0.2	○	0.2	◉	0.8	○	0	▣		○		◉	0.5
	2	p-GaN	○	100	○	200	◉	1.8	○	0	○	1	◉	0	▣		○		◉	1

Main Parameters | Before Active Region | Active Region | After Active Region

Repeat Count	Stage Number	Name	Duration sec	Diffusion layer thickness,cm		Temperature C	Pressure Torr	N2 FlowRate slm	H2 FlowRate slm	NH3 FlowRate slm	TMIn FlowRate,sccm		TMGa FlowRate,sccm		TEGa FlowRate,sccm		TMAl FlowRate,sccm	
											Bub.	Given	Bub.	Given	Bub.	Given	Bub.	Given
10	1	QW	210	1.1	Init	780	350	4	0	-4	□	2.2	□	6	□	0	□	3
					Final	780	350	4	0	-4	□	2.2	□	6	□	0	□	3
	2	barrier	230	1.1	Init	780	350	4	0	4	□	0	□	6	□	0	□	0
					Final	820	350	4	0	4	□	0	□	6	□	0	□	0

Fig. 7.1

7.1 Working with the process stages: general features

Regardless of the position of the particular layer in the heterostructure (within or outside the active region), there are several options that facilitate the procedure of recipe specification:

- There are some operations (grouping, deleting, and copying) that can be applied to several stages. They can be selected by clicking *Shift* + left mouse button.
- Grouping of the stages: recipe of a device heterostructure often includes a sequence of stages (QW+barrier, layers in a superlattice, etc.) that is repeated more than once. Such stages can be specified once and grouped with an assigned number of repetitions. To do this, the user is to select several stages and then press Repeat Count button. Then a dialog window (Fig. 7.2) appears, where it is necessary to set the number of repetitions (***Repeat Count*** field). Another opportunity is to select only one layer form the desired group and then define the stages to be grouped using *From* and *to* boxes. Grouping can be annulled by the same procedure with pressing ***Clear*** button at the end. Layers/stages merged into a group are indicated in the *Repeat Count* column in the recipe table.

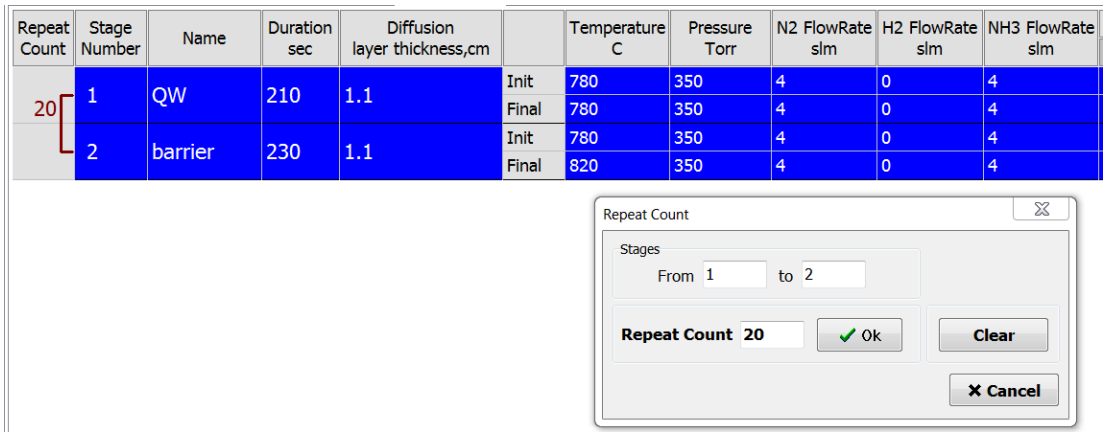

Fig. 7.2

- To append a stage, use Append <Ctrl+Enter> button, a blank line for a new process stage will be added at the end of the stage list.
- One or several stages can be deleted with Delete button.
- To insert an additional line in the recipe before or after the active (marked with dark blue) stage, use Insert Before and Insert After buttons, correspondingly.
- Currently selected process stage can be moved up or down by one position with Move Up and Move Down buttons.

- One or several stages in the recipe can be copied. To do this, the user is to copy the selected stages using 

button, than create a blank line in the proper position of the recipe using the *Append*, *Insert Before* or *Insert After* commands, and paste the selected stages using 

button. The stages selected for copying are marked with a yellow circle 

in the cell with the stage number.

Process parameters specified on ***Before Active Region***, ***Active Region***, and ***After Active Region*** tabs can be exported to an Excel sheet with the 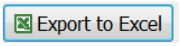

button.

7.2 Stages in the active region

To describe a process stage in the active region, the user is to define the stage name (optional, but recommended item) and duration *(sec)*. Next, it is necessary to specify the transport characteristics. Depending on the option selected in the *Reactor Transport Model* section on the ***Main Parameters*** tab, there are three possibilities:

- If the *Fixed diffusion layer thickness* option was chosen, the boundary layer thickness *(cm)* should be defined for each process stage in the corresponding field;
- If the *Calibration on thick GaN growth rate* option was chosen, there is no need to add any additional information;
- If the *Calibration on average InGaN growth rate and composition* option was chosen, the growth rate and composition should be assigned to each layer in the active region.

Next, the user is to specify the process parameters that include: temperature, pressure, flow rates of N_2, H_2, NH_3, and group-III precursors. Here, two lines (*Init* and *Final*) for these parameters are reserved, thus allowing linear variation of any operating parameter during the particular process stage. When the initial value is introduced, it is automatically copied as the final one, so, for the majority of cases, it is enough to insert the value only once.

It is recommended to avoid strictly stepwise changes in the process parameters between stages. For instance, if a barrier or cap layer (with zero TMIn flow rate) is grown directly after a QW (with some non-zero TMIn flow rate), it is preferable to introduce a short stage where the TMIn flow rate decreases from the value at the QW stage to zero, as represented by “TMIn-off” stage in Fig. 7.3. Adding this stage reflects the fact that the stepwise change of the gas composition at the reactor inlet proves somewhat smoothed when it reaches the growth surface due to the gas species interfusion. Simultaneously, this reduces the stiffness of the problem and improves stability of computations. Another typical case is

temperature variation during the growth; here, the ramping time is normally known and the ramping can be specified as a recipe stage.

Repeat Count	Stage Number	Name	Duration sec	Diffusion layer thickness,cm		Temperature C	Pressure Torr	N2 FlowRate slm	H2 FlowRate slm	NH3 FlowRate slm	TMIn FlowRate,sccm		TMGa FlowRate,sccm		TEGa FlowRate,sccm		TMAl FlowRate,sccm	
											Bub.	Given	Bub.	Given	Bub.	Given	Bub.	Given
10	1	QW	210	1.1	Init	780	350	4	0	4	□	2.2	□	6	□	0	□	3
					Final	780	350	4	0	4	□	2.2	□	6	□	0	□	3
	2	TMIn-off	0.5	1.1	Init	780	350	4	0	4	□	2.2	□	6	□	0	□	3
					Final	780	350	4	0	4	□	0	□	6	□	0	□	3
	3	barrier	230	1.1	Init	780	350	4	0	4	□	0	□	6	□	0	□	0
					Final	820	350	4	0	4	□	0	□	6	□	0	□	0

Fig. 7.3

The MO flow rates can be specified either directly or using bubbler parameters. In the latter case, the bubbler configuration window appears, as shown in Fig. 7.4, after selecting *Bub.* checkbox. The first section of the dialog contains bubbler conditions: flow rate of the carrier gas passing through the bubbler F_{car}, bubbler pressure P, and temperature T.

The second section of the dialog controls the approximation used for the computation of the MO vapor pressure, which is required to compute the MO flow rate. The number of the available approximations depends on the MO species considered; however, there is also *User Defined* item that allows the user to specify custom approximation coefficients. The data for the approximation named *O.Kayser et al*. are taken from paper [8]. The data for the approximation named *Rohm and Haas* were borrowed in the past from the web. Regardless of the selected approximation, the MO vapor pressure P^o (in *Torr* or *mbar,* depending on the source of the approximation data) is computed as $\log(P^o) = -A/T + B$, where the approximation coefficients A and B are either built-in or defined by the user. Eventually, the MO flow rate is computed as $F_{MO} = \dfrac{F_{car}}{P/P^o - 1}$ and displayed in the recipe table after pressing *OK* button.

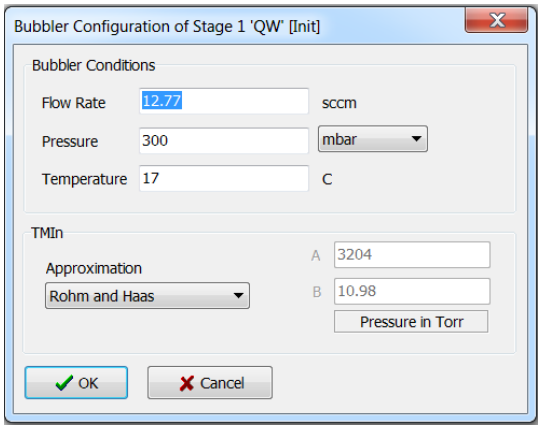

Fig. 7.4

To specify the MO flow rate directly instead of defining it from the bubbler parameters, just deselect the respective checkbox; to view and modify the bubbler parameters, use *Ctrl* + left mouse button.

For control, the process parameters, specified for the active region, are presented graphically at the bottom part of the ***Active Region*** tab. One of the process parameters can be selected for the left axis of the plot (visualized in brown), another one – for the right axis (visualized in blue). The currently active stage in the table is marked on the plot area as a single highlighted zone or several highlighted zones if the stage belongs to a group (see Fig. 7.5 as an example).

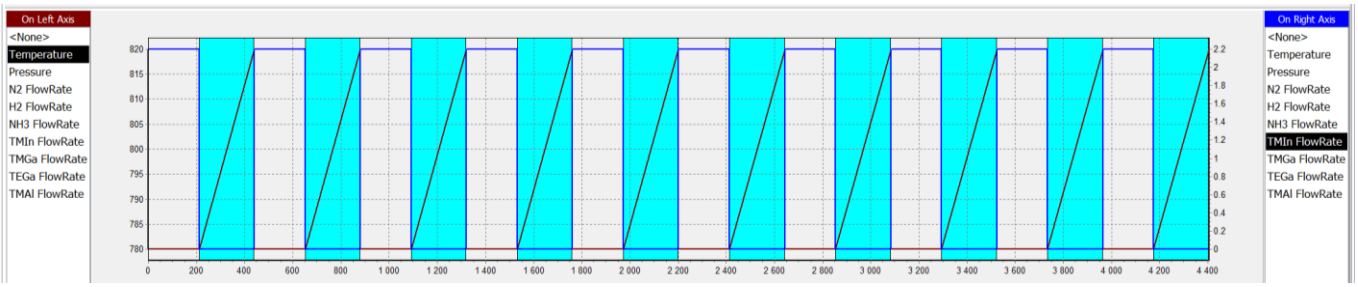

Fig. 7.5

This tool can be helpful for quick checking of the recipe to find possible inaccuracies in the specified process conditions.

Another parameter that may be required for modeling is the dislocation density. Depending on the *Relaxation Model* option and information provided for the layer before the active regions, there are several variants:

- If stress relaxation via V-shaped dislocation half-loops is considered, there is no need to specify the dislocation density in the active region, since this parameter will be computed;
- If stress relaxation is not considered, the dislocation density (*1/cm^2*) for each layer in the active region should be either defined directly or inherited from the previous layer. This is made by selecting the corresponding checkbox in the recipe table, as demonstrated in Fig. 7.6. If there are no layers before the active region, the dislocation density should be specified at least for the first stage in the active region. Actually, when no stress relaxation is assumed, the specified dislocation density does not affect the computed composition profile and serves as supplementary information that can be subsequently used for device modeling with the SiLENSe software.

Dislocation density,1/cm²	
Inherited	Given
☐	1e9
☐	1e9
▣	
▣	
▣	
▣	

Fig. 7.6

7.3 Layers before and after the active region

Since the modeling of composition profile is performed for the active region only, the process parameters for the layers outside it are not required. Instead, four sections should be filled in to specify the layers before and after the active region. The parameters described below are assumed to remain unchanged within each layer outside the active region.

- *Thickness characteristics*: here, three parameters are available for editing: *Thickness*, *Duration*, and *Growth rate*; the user is to define an arbitrary pair of them, while the third one is automatically restored. The latter parameter is indicated by *Calc* radio button in the respective column, and this field is marked with green, as displayed in Fig. 7.7. The two other parameters are inserted into the *Given* field of the respective columns.

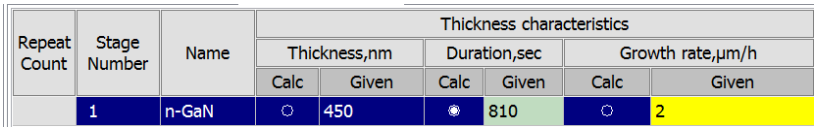

Fig. 7.7

If the user changes the growth rate unit in the *Units* section on the ***Main Parameters*** tab, the table for the layers before and after the active region is automatically renewed in the following way: (i) if the growth rate is the given parameter, its value remains the same, but the calculated value changes due to the different unit of the growth rate; (ii) if the growth rate is the calculated parameter, its value changes, but the two other parameters remain the same. The user is informed about the changes with the warning window shown in Fig. 7.8;

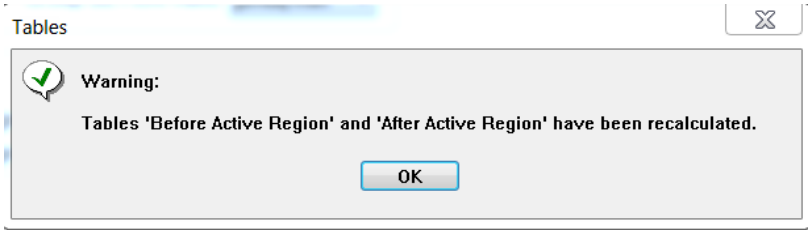

Fig. 7.8

- *Composition*: similarly to the thickness characteristics, the layer composition is defined by the content of any two constituents of an InGaAlN layer, for the remaining constituent, the content is recalculated form the condition of the unity total content;
- *Dislocation density*: can be specified directly or inherited from the previous layer; for the first layer before the active region, the dislocation density should be defined explicitly;
- *Stress state*: one of the purposes of including layers before the active region is to specify the lattice constant of the layer underlying the active region to subsequently use this value for lattice mismatch

and strain computations. The stress sate can be defined either via the *a* lattice constant (*Å*) or via the relaxation degree. The relaxation degree serves to find the effective lattice constant of the layer and is determined as $r = \frac{a^{eff}_{current} - a^{eff}_{previous}}{a^{bulk}_{current} - a^{eff}_{previous}}$, where $a^{eff}_{current}$ and $a^{eff}_{previous}$ are the effective lattice constants of the current and previous layers, respectively, and $a^{bulk}_{current}$ is the lattice constant of the bulk (fully relaxed) material. Thus, for the first layer in the heterostructure, only the lattice parameter can be specified.

The lattice parameters of the binary materials, used in the STREEM-InGaN software, are summarized in Table 7.1. Vegard's low is applied to compute the lattice parameters for ternary and quaternary layers.

Material	**a, Å**
AlN	3.112
GaN	3.189
InN	3.54

Table 7.1

Example of layers before the active region is shown in Fig. 7.9: thick p-GaN is followed by a relaxed $In_{0.08}Ga_{0.92}N$ underlayer whose lattice parameter will be used in the active region (more details on the role of underlayers can be found in the description of Example 4, Section 9).

Name	Thickness characteristics						Composition						Dislocation density 1/cm²		Stress state			
	Thickness,nm		Duration,sec		Growth rate,μm/h		AlN		GaN		InN							
	Calc	Given	Calc	Given	Calc	Given	Calc	Given	Calc	Given	Calc	Given	Inherited	Given	Used	a,Å	Used	Relax.Degree
n-GaN	◉	450	○	810	○	2	◉	0	○	1	○	0	☐	1e10	◉	3.189	○	
underlayer	○	150	◉	2700	○	0.2	◉	0	○	1	○	0	☐	1e10	○		◉	1

Fig. 7.9

Lattice constant or relaxation degree for the layers after the active region can be specified in the same way. If the relaxation degree is defined for a layer after the active region, the effective lattice constant at the end of the active region growth is used as that of the previous layer. The effective lattice constant is one of the variables available during visualization of the results, as discussed in the next Section.

Note that the layers before and after the active region can be omitted in the recipe. In this case, the active region is assumed to grow on a thick relaxed GaN.

8. Running the computations and viewing the results

To run the computations, press 

button that is available in the bottom section of ***Main Parameters, Before Active Region***, ***Active Region***, and ***After Active Region*** tabs. The solver progress is depicted with 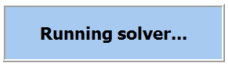

window. In case of any solver errors, a window appears as shown in Fig. 8.1. The most probable solver error is too small time step. If so, a possible solution may be modifying the recipe to avoid stepwise changes in the process parameters as discussed in Section 7. In case of normal termination of the solver, the user is informed about this and redirected to the ***STREEM Results*** tab (see Fig. 8.1). Modeling results are stored in the ***project_name.dat*** file and loaded automatically for visualization on the ***STREEM Results*** tab.

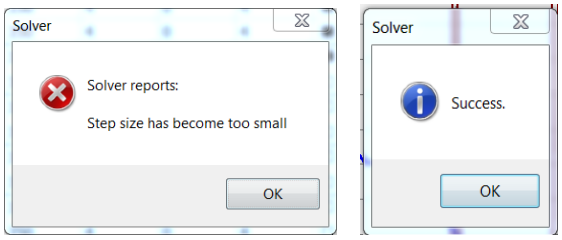

Fig. 8.1

Results of the computations are visualized in form of one-dimensional plots. As the x-axis variable, the user can select either *time (sec)* or interface coordinate *z (nm)* from *Argument* drop-down menu. Each plot may have one or two y-axes, and the dependent variable for the left and right axis is selected form the respective sections on the ***STREEM Results*** tab as shown in Fig 8.2. Brown and blues curves represent the left-axis variable and the right-axis one, correspondingly. Up to five charts can be displayed simultaneously; the number of charts is selected with 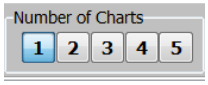

section.

To adjust the label format for any particular variable, use one of 

buttons and then select the format from the available list as demonstrated in Fig. 8.3.

The numerical technique implemented in the STREEM-InGaN software utilizes automatic adaptation of time steps, and it is possible to follow time step variation during the computations. For this purpose, points can be added on the plots, using 

section on the ***STREEM Results*** tab. The first button is to display lines only; the other buttons correspond to the points of different size on the plots.

Close location of points over some part of the curve means that the solver had to reduce the time step considerably due to steep gradients of some variables.

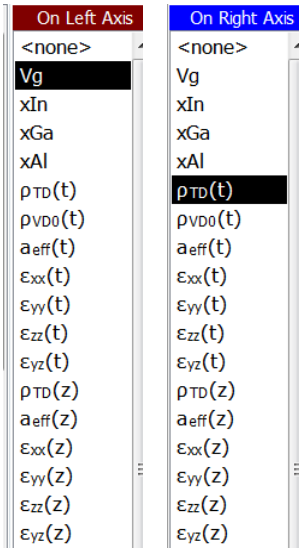

Fig. 8.2

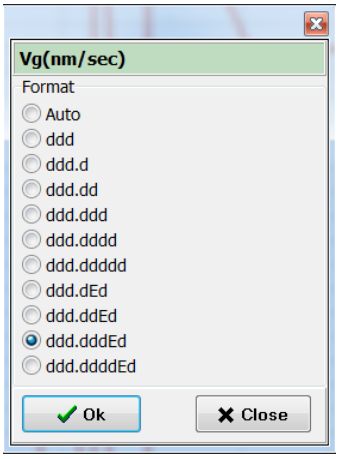

Fig. 8.3

At any cursor position on the chart field, the user can see the values of the x-axis and y-axes variables above the plot area: time(sec)=7474.2 Vg=0.0162 xIn=0.03466. For better representation of the probe position, press button.

To zoom in a part of the graph, select the area of interest on the chart by pressing the left mouse button and dragging the mouse to a diagonal corner of the desired area, the overall direction should be left-to-right; the selected area will be represented by a black rectangle. To zoom out, drag the mouse in the opposite direction or press Undo Zoom button.

To set manually the axis ranges for both the argument and dependent variables, use Argument, Left Axis, and Right Axis buttons from the *Min Max* section and specify the minimum/maximum values in the dialog window as shown in Fig. 8.4. To fit ranges to the full size, press the Auto button.

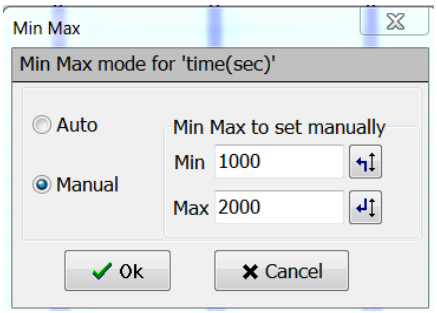

Fig. 8.4

Each chart field can be exported into an image file by pressing Save Chart button and further selection of the file format and name in a standard dialog window.

For each chart, the currently displayed variables can be exported to an Excel sheet with Excel button. All computational results can be exported by pressing All Variables to Excel button.

Since the actual composition profile and thicknesses of individual layers in the heterostructure are different from the nominal values due to the surface segregation effects and stress relaxation, it is important to distinguish particular stages of the recipe in the plots. For this purpose, all layers from the recipe are listed in the *Layers* section on the ***STREEM Results*** tab. By activating Color Each checkbox, it is possible to associate the layers, having the same name, with particular color. One or several layers can be selected by toggling corresponding checkboxes. Fig. 8.5 shows an example where all quantum wells in the structure are selected. If so, the selected layers are marked on the chart area with highlighted zones which are either cyan (if the *Color Each* checkbox is inactive) or have the color specific for this group of layers. Example of visualization with layers highlighted in both ways is given in Fig. 8.6. Note that an arbitrary number of layers with arbitrary names (ultimately, all layers) can be highlighted at a time. The buttons in the *Selection* section are to select all layers, deselect all layers, and invert selection *.

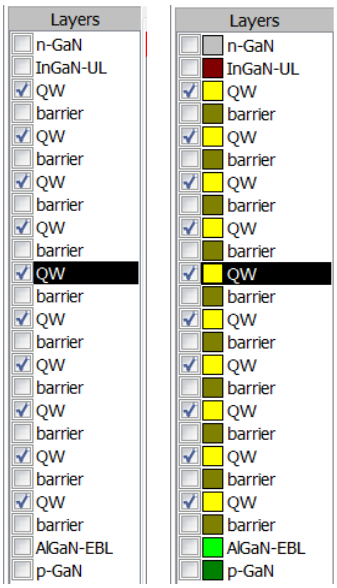
Layers
n-GaN
InGaN-UL
QW
barrier
QW
barrier
QW
barrier
QW
barrier
QW
barrier
QW
barrier
QW
barrier
QW
barrier
QW
barrier
AlGaN-EBL
p-GaN
Layers
n-GaN
InGaN-UL
QW
barrier
QW
barrier
QW
barrier
QW
barrier
QW
barrier
QW
barrier
QW
barrier
QW
barrier
QW
barrier
AlGaN-EBL
p-GaN

Fig. 8.5

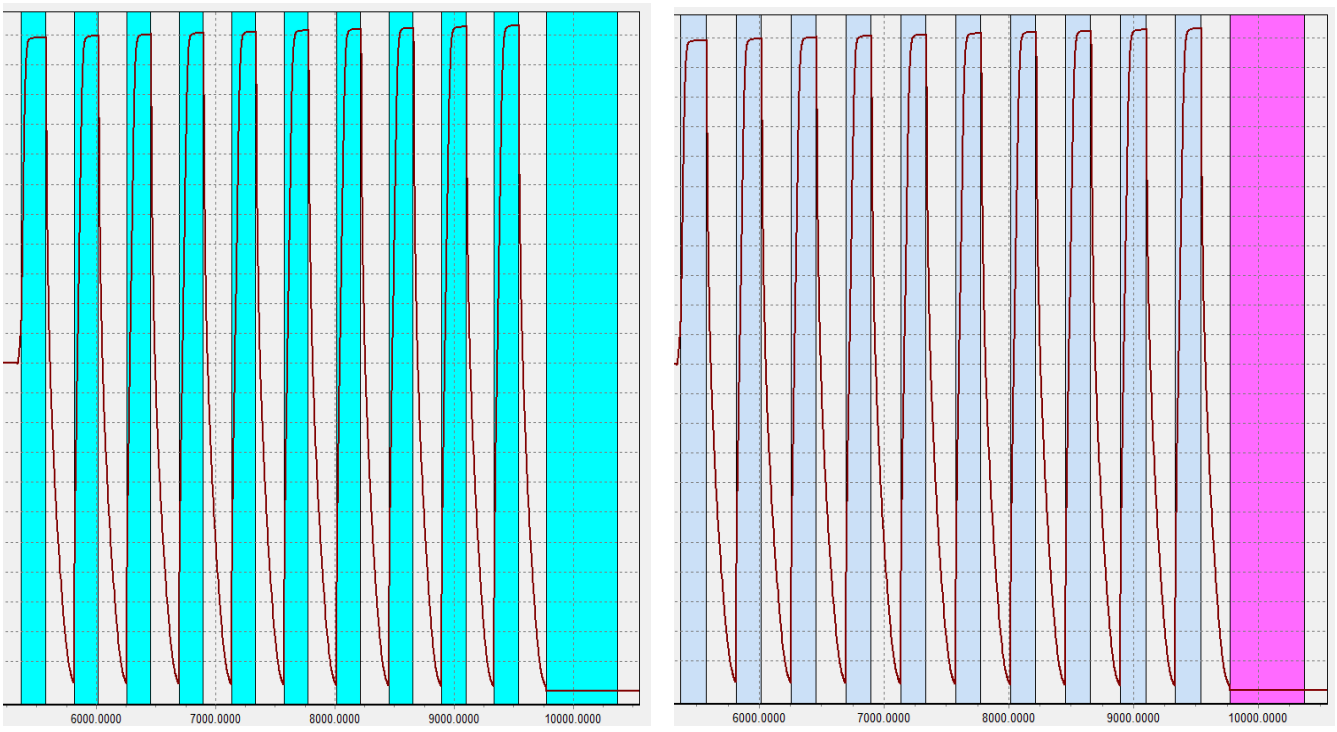
6000.0000
7000.0000
8000.0000
9000.0000
10000.0000
6000.0000
7000.0000
8000.0000
9000.0000
10000.0000

Fig. 8.6

The list of dependent variables with the respective units is given in Table 8.1.

Variable	Meaning	Unit
Vg	growth rate	*nm/sec*
xIn, xGa, xAl	layer composition	-
$\rho_{TD}(t)$	threading dislocation density vs time	cm^{-2}
$\rho_{VD0}(t)$	the density of the V-dislocations at the apex vs time	cm^{-2}
$a_{eff}(t)$	effective lattice constant vs time	*Å*
$\varepsilon_{xx}(t), \varepsilon_{yy}(t), \varepsilon_{zz}(t), \varepsilon_{yz}(t)$	strain tensor components vs time	-
$\rho_{TD}(z)$	threading dislocation density vs thickness	cm^{-2}
$a_{eff}(z)$	effective lattice constant vs thickness	*Å*
$\varepsilon_{xx}(z), \varepsilon_{yy}(z), \varepsilon_{zz}(z), \varepsilon_{yz}(z)$	strain tensor components vs thickness	-

Table 8.1

The effective lattice constant is computed as $a_{eff} = a^{bulk} \cdot \left(\varepsilon_e + \varepsilon_p + 1\right)$, where a^{bulk} is the lattice constant of bulk InGaAlN with the composition *xIn, xGa*, and *xAl*, $\varepsilon_e(z) = \frac{a_s - a^{bulk}}{a^{bulk}}$ is the elastic deformation (a_s is the latticed parameter of the underlying layer), and ε_p is the plastic deformation that depends on the dislocation density. Until stress relaxation occurs, the effective lattice constant remains unchanged and equal to a_s, in the opposite ultimate case of a fully relaxed layer, $a_{eff} = a^{bulk}$.

For [0001] growth direction, the strain tensor components are: $\varepsilon_{xx} = \varepsilon,\ \varepsilon_{yy} = \varepsilon,\ \varepsilon_{zz} = -2\frac{C_{13}}{C_{33}}\varepsilon,\ \varepsilon_{yz} = 0$, where $\varepsilon = \frac{a^{eff} - a^{bulk}}{a^{bulk}}$ is the total deformation and C_{ij} are the elastic constants.

It is important to note that the dislocation density, effective lattice constant, and strain tensor components are included into the list of variables as functions of both time and thickness. All characteristics of the heterostructure are primarily found in STREEM-InGaN as functions of time. For each moment of time t_i, $z(t_i)$ is the local coordinate of the upper interface of the heterostructure at that time. This means that the distributions of any variable versus time and coordinate represent the evolution of *in-situ* values of this variable and are formed as t_i, $z(t_i)$, $value(t_i)$.

However, from practical point of view, it is also important to know resulting distributions of the above

characteristics across the structure **after** the structure growth. For instance, measurements of the lattice parameter with XRD or observations of dislocations with TEM are normally performed after the growth. Modeling of device operation also requires spatial rather than temporal variations of the heterostructure characteristics. Thus, the final distributions of some variables versus thickness are additionally introduced in the STREEM-InGaN.

The main reason for differences between the temporal (in-situ) and spatial (resulting) variations comes from the behavior of the dislocations. As discussed in Section 3 and references cited there, new dislocation half-loops are produced during the growth, but, being generated, they instantly penetrate down, as a rule, to the (Al)InGaN/GaN interface (the apex coordinate z_0 is found during the computations). Even in case of relaxation of a single thick InGaN layer, the distributions of the $\rho_{TD}(t)$ (brown curve) and $\rho_{TD}(z)$ (blue curve) are different, as shown in Fig. 8.7 with reference to conditions applied in Example 5: while $\rho_{TD}(z)$ has a maximum at the InGaN/GaN interface and then decreases due to annihilation of dislocations, $\rho_{TD}(t)$ increases, reaches some maximum value and then decreases. Both distributions are the same, starting from some coordinate (moment of time) when new dislocations no longer appear, and only annihilation takes place.

Following the dislocation density, the related characteristics, such as the effective lattice constant and strain, also have different distributions versus time and thickness when stress relaxation occurs. In contrast, the distribution of the layer composition versus time and thickness are similar, as the chemical composition may change only locally and these changes do not affect the layers underneath.

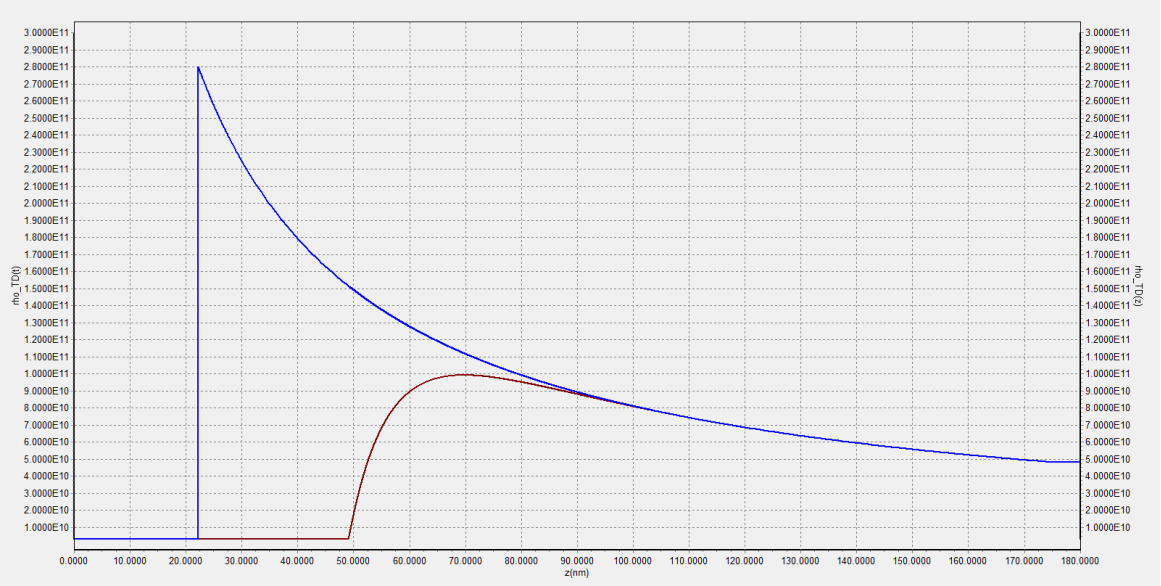

Fig. 8.7

By default, the results of the current computation are visualized. Results, corresponding to other projects, can be loaded using 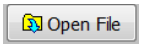

button on the ***STREEM Results*** tab.

STREEM-InGaN output file ***project_name.dat*** can be directly imported into the SiLENSe software. The composition, strain, and dislocation density distributions computed within the STREEM-InGaN will be applied for the modeling of LED characteristics with the SiLENSe.

Parameters that the user has adjusted while analyzing the results (number of plots, argument and dependent variables, axis ranges, label format, etc.) are stored as GUI settings and will be used in all subsequent launchings of the GUI, until any changes are introduced.

9. Examples

The examples below illustrate the application of the STREEM-InGaN software to the analysis of the influence of indium surface segregation, process parameters, stress relaxation, thick InGaN undelayers, and including AlGaN into barrier layers on the resulting characteristics of InGaN-based heterostructures. The examples are stored in the *Examples* folder. To see the main parameters and recipes, load the ***project_name.stm*** file from the respective sub-folder (*Example1÷Example7*), to see the computational results, run the computation or load the result file ***project_name.dat***.

9.1 Example 1: segregation effects in SQW structure

The example considers a rather simple case when the growth of an InGaN QW is followed by the growth of a GaN barrier layer. Here, the project files ***SQW.stm*** and ***SQW_no_segregation.stm*** correspond to the computation with the segregation effect and with *No Segregation* option in the *Segregation Model* section on the ***Main Parameters*** tab. Parameters of GaN growth in a vertical high-speed rotating disk reactor are specified as reference ones (see *Reactor Transport Model* section). Figs. 9.1-9.2 allow one to understand the effect of the indium surface segregation on the indium composition profile (nominal QW region is marked with cyan): while the computation with no segregation demonstrates a rectangular QW (Fig. 9.1), the computation considering this effect (Fig. 9.2) predicts an indium tail in the barrier after TMIn supply is terminated.

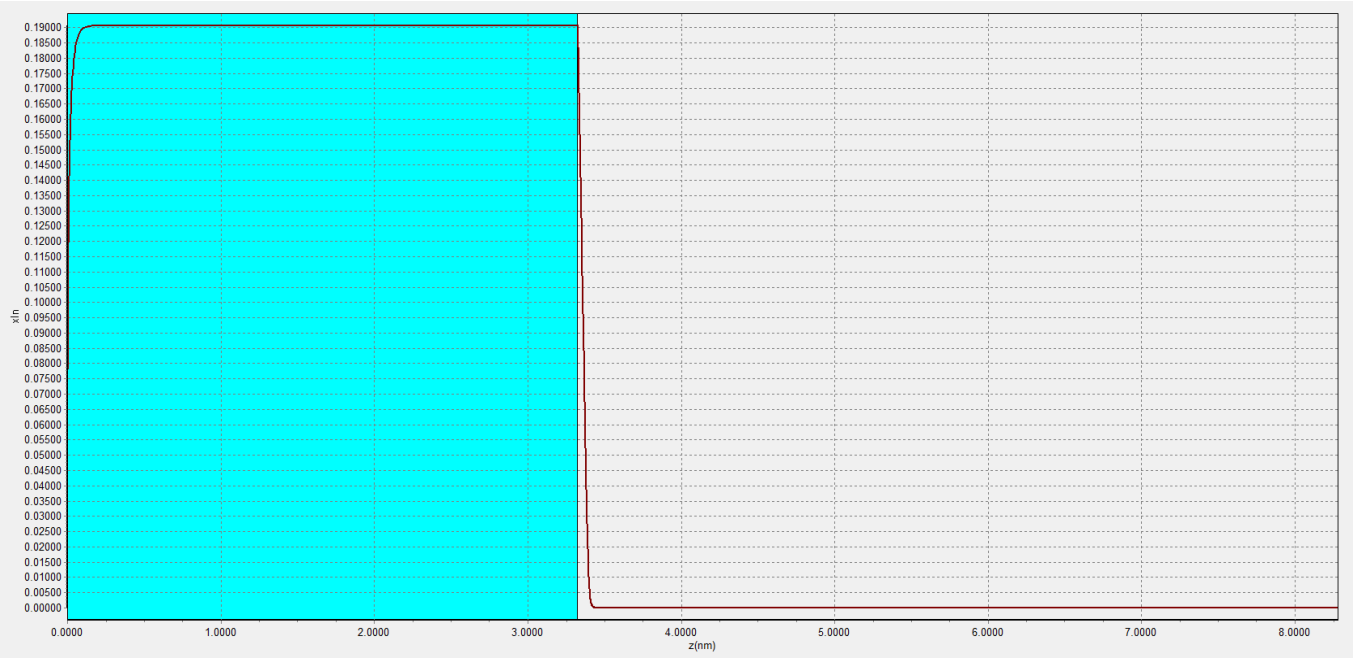

Fig. 9.1

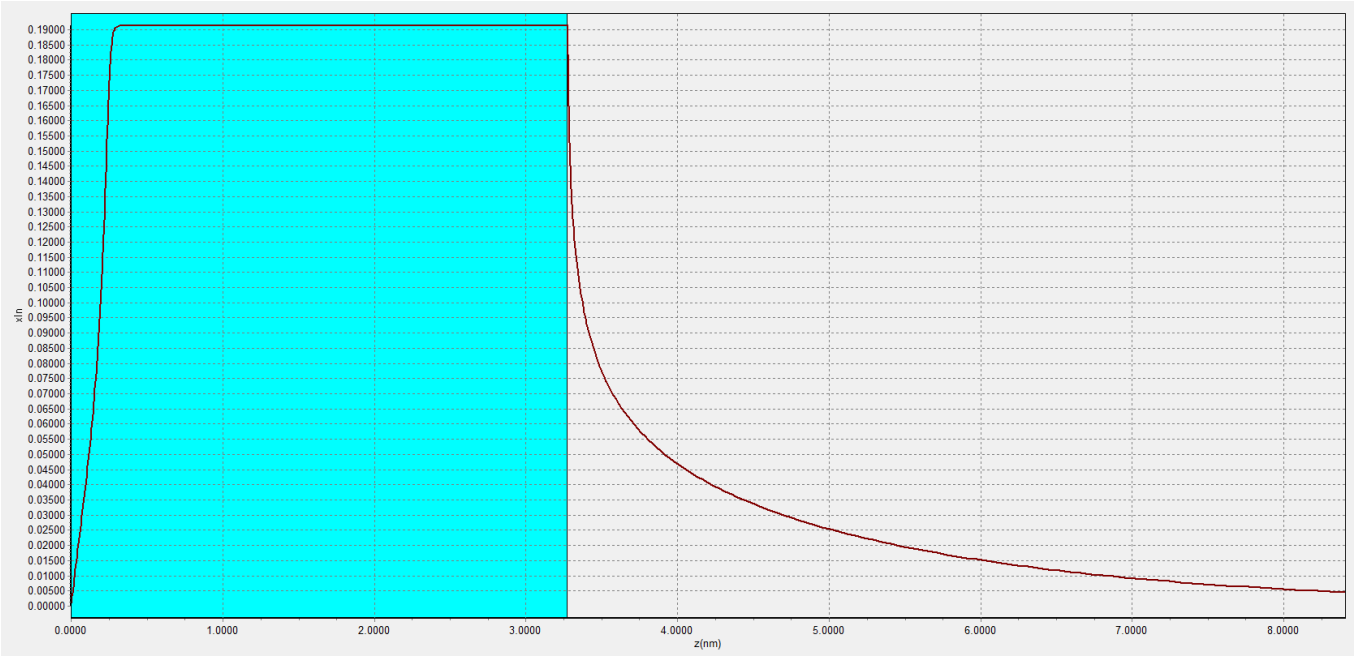

Fig. 9.2

9.2 Example 2: effect of process parameters on indium composition profile in MQW structure with moderate indium content

The example illustrates the effect of process parameters on the indium incorporation and composition profile across a MQW InGaN/GaN structure. Growth of five InGaN QWs separated by GaN barriers is considered. As the transport model, the diffusion layer thickness is directly specified for the stages in the active region. The reference process parameters (corresponding to the 2nd QW) are similar to those presented in Ref [3]:

- InGaN QW growth temperature – 750 °C;
- GaN cap growth temperature – 750 °C;
- GaN barrier growth temperature – 920 °C;
- Total pressure – 200 Torr;
- TMIn flow rate – 0.4 sccm;
- TEGa flow rate – 0.8 sccm;
- NH_3 flow rate – 30 slm;
- N_2 flow rate – 60 slm;
- QW growth duration – 75÷90 sec;
- Barrier growth duration – 180 sec.

The stages of QW and barrier growth (*QW_Growth* and *Barrier_Growth*, respectively) are separated by the intermediate stages of GaN cap growth (*Cap_Growth*, 180 sec), temperature ramping (*T_RampUp* and *T_RampDown*, 90 sec), and temperature stabilization (*T_Stab*, 90 sec). In addition, for better computation stability, each QW growth stage is separated from the previous and next stages by very short stages of TMIn switching-on and -off (*In_RampUp* and *In_RampDown*, 1 sec). A part of the recipe table, corresponding to reference period of the MQW structure, is given in Fig. 9.3.

Repeat Count	Stage Number	Name	Duration sec	Diffusion layer thickness,cm
	9	In_RampUp	1	0.325
	10	QW_Growth	90	0.325
	11	In_RampDown	1	0.325
	12	Cap_Growth	180	0.325
	13	T_RampUp	90	0.325
	14	Barrier_Growth	180	0.325
	15	T_RampDown	90	0.325
	16	T_Stab	90	0.325

	Temperatu C	Pressure Torr	N2 FlowRa slm	H2 FlowRa slm	NH3 Flowf slm	TMIn FlowRate,sccm Bub	TMIn FlowRate,sccm Given	TMGa FlowRate,sccm Bub.	TMGa FlowRate,sccm Given	TEGa FlowRate,sccm Bub.	TEGa FlowRate,sccm Given	TMAl FlowRate,sccm Bub.	TMAl FlowRate,sccm Given
Init	750	200	60	0	30	☐	0	☐	0	☐	0.8	☐	0
Final	750	200	60	0	30	☐	0.4	☐	0	☐	0.8	☐	0
Init	750	200	60	0	30	☐	0.4	☐	0	☐	0.8	☐	0
Final	750	200	60	0	30	☐	0.4	☐	0	☐	0.8	☐	0
Init	750	200	60	0	30	☐	0.4	☐	0	☐	0.8	☐	0
Final	750	200	60	0	30	☐	0	☐	0	☐	0.8	☐	0
Init	750	200	60	0	30	☐	0	☐	0	☐	0.8	☐	0
Final	750	200	60	0	30	☐	0	☐	0	☐	0.8	☐	0
Init	750	200	60	0	30	☐	0	☐	0	☐	0.8	☐	0
Final	920	200	60	0	30	☐	0	☐	0	☐	0.8	☐	0
Init	920	200	60	0	30	☐	0	☐	0	☐	0.8	☐	0
Final	920	200	60	0	30	☐	0	☐	0	☐	0.8	☐	0
Init	920	200	60	0	30	☐	0	☐	0	☐	0.8	☐	0
Final	750	200	60	0	30	☐	0	☐	0	☐	0.8	☐	0
Init	750	200	60	0	30	☐	0	☐	0	☐	0.8	☐	0
Final	750	200	60	0	30	☐	0	☐	0	☐	0.8	☐	0

Fig. 9.3

Within the example, the following parameters are varied as compared to the reference case:

- Temperature of InGaN QW growth – 715 °C (1st QW);
- Temperature of GaN cap layer – 750-920 °C (3rd QW);
- TMIn flow rate – 0.7 sccm (4th QW);
- TEGa flow rate – 0.4 sccm (5th QW).

The corresponding In content profile computed with the software is presented in Fig. 9.4. Here, the nominal InGaN QW growth stages, GaN cap growth stages, and temperature ramping stages are shown in brown, pink, and blue colors, respectively; the other stages are not indicated with any color.

It is seen from the figure that the computed In content profile essentially differs from the nominal one. In particular, it exhibits abrupt but still somewhat sloped fore fronts and considerably sloped rear fronts, so that rather long indium tails prove incorporated into the GaN barriers. Depending on the process parameters, the computed profile demonstrates the following effects:

- Decrease of InGaN QW growth temperature from 750 °C to 715 °C results in increase of the In content from ~16% to ~23% (2nd reference QW vs. 1st QW);
- Shortening of the low-temperature (750 °C) part of GaN cap growth stage from 180 sec to 30 sec provides shortening of the In “tail” in the barrier from ~4 nm to ~2 nm (3rd QW vs. reference 2nd QW);

- Rise of TMIn flow rate from 0.4 sccm to 0.7 sccm results in increase of the In content from ~16% to ~20% (4th QW vs. reference 2nd QW);
- Decrease of TEGa flow rate from 0.8 sccm to 0.4 sccm leads to almost proportional shortening of the InGaN QW thickness, from ~2 nm to ~1 nm, but weakly affects the In incorporation (5th QW vs. reference 2nd QW).

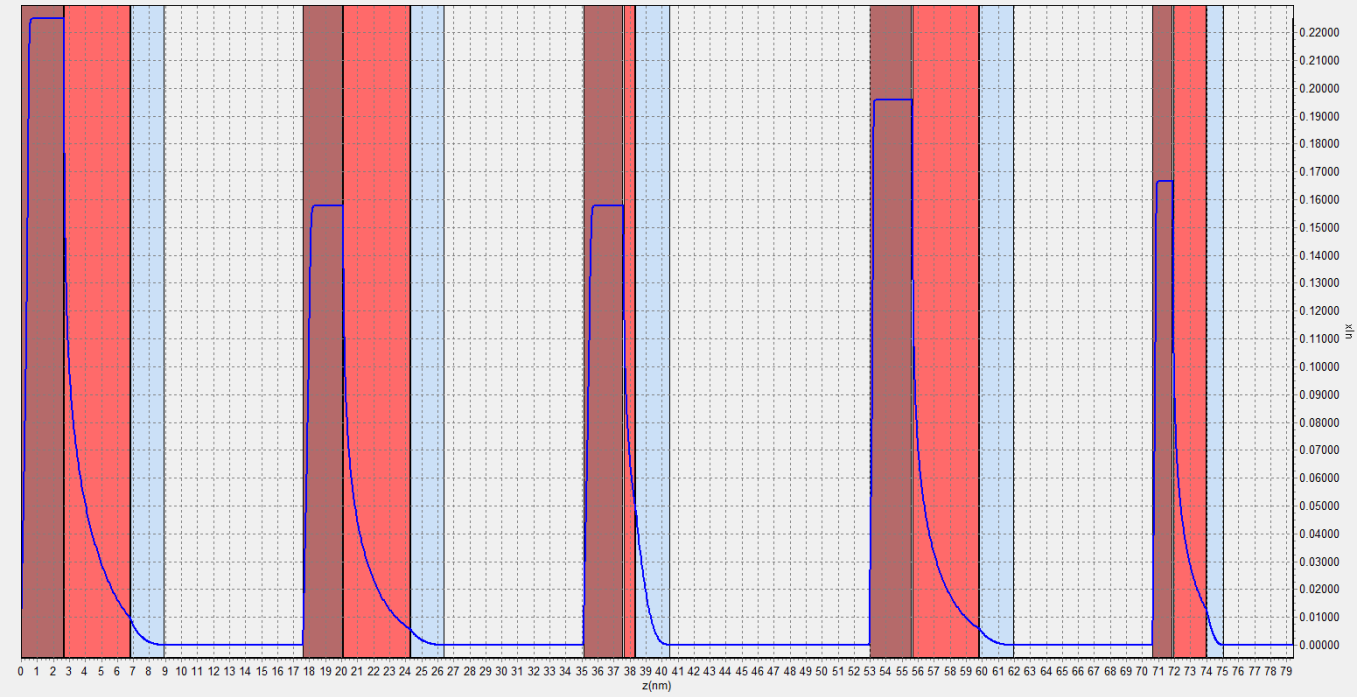

Fig. 9.4

9.3 Example 3: MQW structure with stress relaxation

The so called 'green gap' in the efficiency of III-nitride light-emitting diodes and laser diodes is frequently attributed, at least in part, to intensive generation of extended defects during stress relaxation in active (0001)InGaN quantum wells grown on thick GaN buffer/contact layers. In the following example case, a MQW structure is analyzed with respect to stress relaxation in the active region and respective changes in the indium composition profile. The structure is similar to that reported in Refs. [9-10], and the active region consists of five periods, each of them includes the following stages: quantum well, cap layer, growth interruption accompanied by temperature ramping from T_{QW} to $T_{barrier}$, barrier, and the second temperature ramping (from $T_{barrier}$ back to T_{QW}). The process conditions are applicable to AIX2000HT planetary reactor, and calibration on thick GaN growth is used. The process conditions for one period of the recipe are given in Fig. 9.5.

Repeat Count	Stage Number	Name	Duration sec		Temperature C	Pressure mbar	N2 FlowRate slm	H2 FlowRate slm	NH3 FlowRate slm	TMIn FlowRate,sccm		TMGa FlowRate,sccm		TEGa FlowRate,sccm		TMAl FlowRate,sccm	
										Bub.	Given	Bub.	Given	Bub.	Given	Bub.	Given
5	1	MO-on	0.5	Init	685	200	10	0	23	☐	0	☐	0	☐	0	☐	0
				Final	685	200	10	0	23	▣	0.64048	☐	0	▣	0.41343	☐	0
	2	QW	60	Init	685	200	10	0	23	▣	0.64048	☐	0	▣	0.41343	☐	0
				Final	685	200	10	0	23	▣	0.64048	☐	0	▣	0.41343	☐	0
	3	TMIn-off	0.5	Init	685	200	10	0	23	▣	0.64048	☐	0	▣	0.41343	☐	0
				Final	685	200	10	0	23	☐	0	▣	1.0459	☐	0	☐	0
	4	cap	14	Init	685	200	10	0	23	☐	0	▣	1.0459	☐	0	☐	0
				Final	685	200	10	0	23	☐	0	▣	1.0459	☐	0	☐	0
	5	MO-off	0.5	Init	685	200	10	0	23	☐	0	▣	1.0459	☐	0	☐	0
				Final	685	200	10	0	23	☐	0	☐	0	☐	0	☐	0
	6	ramping-up	40	Init	685	200	10	0	23	☐	0	☐	0	☐	0	☐	0
				Final	750	200	10	0	23	☐	0	☐	0	☐	0	☐	0
	7	TMGa-on	0.5	Init	750	200	10	0	23	☐	0	☐	0	☐	0	☐	0
				Final	750	200	10	0	23	☐	0	▣	1.0459	☐	0	☐	0
	8	barrier	200	Init	750	200	10	0	23	☐	0	▣	1.0459	☐	0	☐	0
				Final	750	200	10	0	23	☐	0	▣	1.0459	☐	0	☐	0
	9	TMGa-off	0.5	Init	750	200	10	0	23	☐	0	▣	1.0459	☐	0	☐	0
				Final	750	200	10	0	23	☐	0	☐	0	☐	0	☐	0
	10	ramping-down	40	Init	750	200	10	0	23	☐	0	☐	0	☐	0	☐	0
				Final	685	200	10	0	23	☐	0	☐	0	☐	0	☐	0

Fig. 9.5

The example includes two project files: ***MQW_no_relaxation.stm*** one is for *No Relaxation* option, ***MQW_with_relaxation.stm*** one is for *V-dislocations* option in the *Relaxation Model* section. To model the indium surface segregation, the "standard" approach with no site blocking effect is applied, which seems preferable for the structures with enhanced indium content.

Fig. 9.6 presents the indium content distribution in the active regions. When the stress relaxation is ignored (*No Relaxation* option), the indium content remains the same, regardless the number of QWs. The account of stress relaxation via formation of V-shaped dislocation HLs (*V-dislocations* option) modifies the composition profile: the stress relaxation occurs after the second QW, and the indium incorporation increases subsequently in the 3rd-5th quantum wells. This results correlates with experimental data which demonstrate an increase in the emission wavelength and indium content as the number of QWs is raised from one to five.

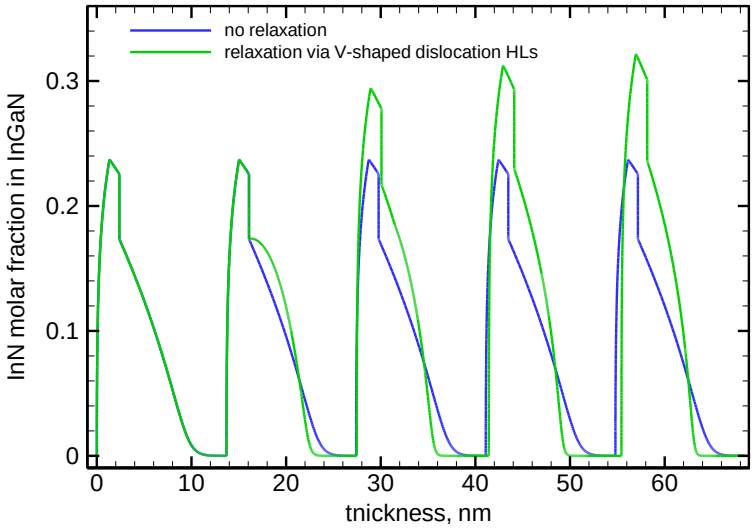

Fig. 9.6

9.4 Example 4: effect of InGaN underlayers

The use of InGaN underlayers (UL) and InGaN/GaN superlattices is now actively exploited during the growth of III-Nitride LED structures for strain balancing in the active regions of heterostructures. Addition an InGaN layer under the MQW stack was shown to improve the efficiency of the MQWs. The example below demonstrates how the effect of ULs can be interpreted within the STREEM-InGaN software.

This example considers the growth of so-called strain balanced multiple quantum well (SBMQW) structures consisting of ten $In_xGa_{1-x}N$(4nm)/GaN(4nm) periods grown on 180 nm thick $In_yGa_{1-y}N$ UL for x>y [11]. According to [11], the $In_yGa_{1-y}N$ ULs are fully relaxed. The SBMQW active region implies that x=2y, if the wells and barriers have the same thickness. Indium composition in the quantum wells was controlled by changing the growth temperature. Since process parameters are not exactly known, a GaN growth regime in the 3x2" close-coupled showerhead reactor is chosen as the reference.

$In_xGa_{1-x}N$/GaN MQW structures with x=16% and x=22% grown on $In_yGa_{1-y}N$ underlayers with y=8% and y=11%, respectively, are compared to the conventional structures without UL. The project files ***InGaN-UL-x0.08.stm*** and ***InGaN-UL-x0.11.stm*** are for the ULs with y=8% and y=11%, files ***InGaN-x0.08.stm*** and ***InGaN-x0.11.stm*** are for the same structures without ULs. The structure begins with an n-GaN layer, and is supplemented with partly relaxed AlGaN blocking layer and p-GaN one after the active region. To account for generation of V-shaped dislocation HLs and annihilation of threading dislocations (both new and those coming from the layers underneath the active region), InGaN UL is introduced into the active region. Process recipe for the active region is presented in Fig. 9.7 for y~11%. Throughout the computations, the *V-dislocations* option was selected in the *Relaxation Model* section.

Repeat Count	Stage Number	Name	Duration sec		Temperature C	Pressure Torr	N2 FlowRate slm	H2 FlowRate slm	NH3 FlowRate slm	TMIn FlowRate,µmol/min		TMGa FlowRate,µmol/min		TEGa FlowRate,µmol/min		TMAl FlowRate,µmol/min	
										Bub.	Given	Bub.	Given	Bub.	Given	Bub.	Given
	1	InGaN_UL	4800	Init	790	350	4	0	4	▣	1.8958	▣	12.456	□	0	□	0
				Final	790	350	4	0	4	▣	1.8958	▣	12.456	□	0	□	0
	2	ramping	30	Init	790	350	4	0	4	□	0	□	0	□	0	□	0
				Final	745	350	4	0	4	□	0	□	0	□	0	□	0
	3	MO-on	1	Init	745	350	4	0	4	□	0	□	0	□	0	□	0
				Final	745	350	4	0	4	▣	2.2008	□	6.0037	□	0	□	0
10	4	QW	210	Init	745	350	4	0	4	▣	2.2008	▣	6.0037	□	0	□	0
				Final	745	350	4	0	4	▣	2.2008	▣	6.0037	□	0	□	0
	5	barrier	230	Init	745	350	4	0	4	□	0	▣	6.0037	□	0	□	0
				Final	745	350	4	0	4	□	0	▣	6.0037	□	0	□	0

Fig. 9.7

The modeling predicts full relaxation of 180 nm underlayers, which allows the subsequent growth of a ten period MQW structure with about the same indium composition profile across the quantum wells and no additional stress relaxation. In contrast, stress relaxation after several starting QWs, formation of new dislocations in the active region, and changes in the In content distribution in the subsequent QWs are predicted for the structures without UL, as demonstrated in Fig. 9.8 (a-b) for the active region of the structures with different indium content.

Variation of the threading dislocation density in the structures is shown in Fig. 9.8 (c-d). New dislocations are generated in the ULs, but the dislocation density drops considerably due to annihilation and keeps reducing in the MQW region. On the contrary, generation of new dislocations in the MQW region is predicted for the structures without ULs, and, eventually, the dislocation density is significantly higher, if no underlayer is grown.

These findings are in agreement with the data given in [11]. In particular, the authors report that the ten period structures can be grown without relaxation-related effects, using the SBMQW growth technique.

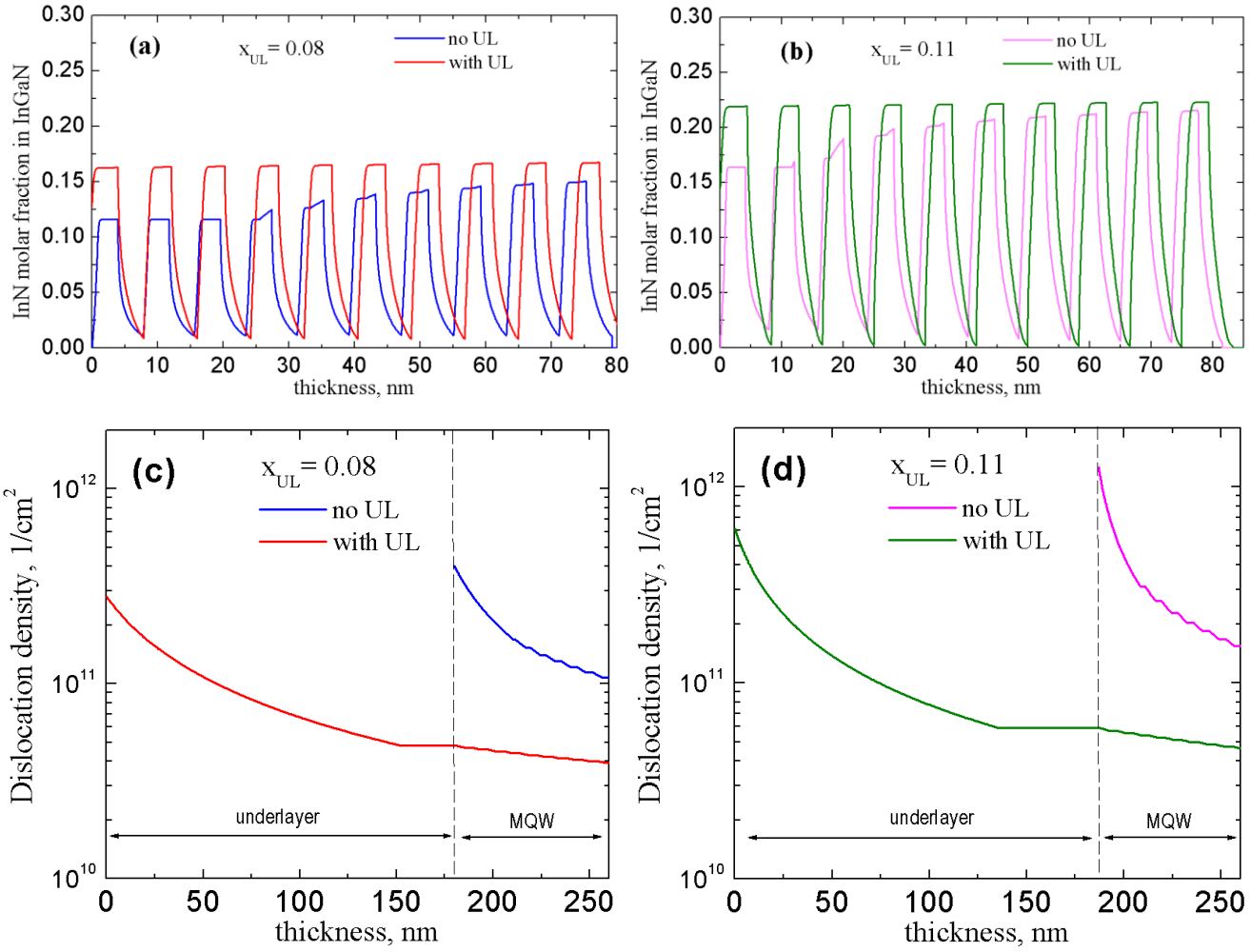

Fig. 9.8

9.5 Example 5: relaxation of thick InGaN layer

The previous example case includes a 180 nm thick fully relaxed InGaN UL before the active region. The authors of [11] claim that the ULs with the thickness of 80 nm did not relax completely, while

160 nm and 180 nm thick ULs were relaxed. The results presented in Fig. 9.9 agree with these observations: InGaN layer with the initial indium content of about 6 % starts to relax at the thickness of about 30 nm (in agreement with the data on the critical thickness vs composition from [6]) and reaches the constant composition of about 8 % when its thickness exceeds 150 nm.

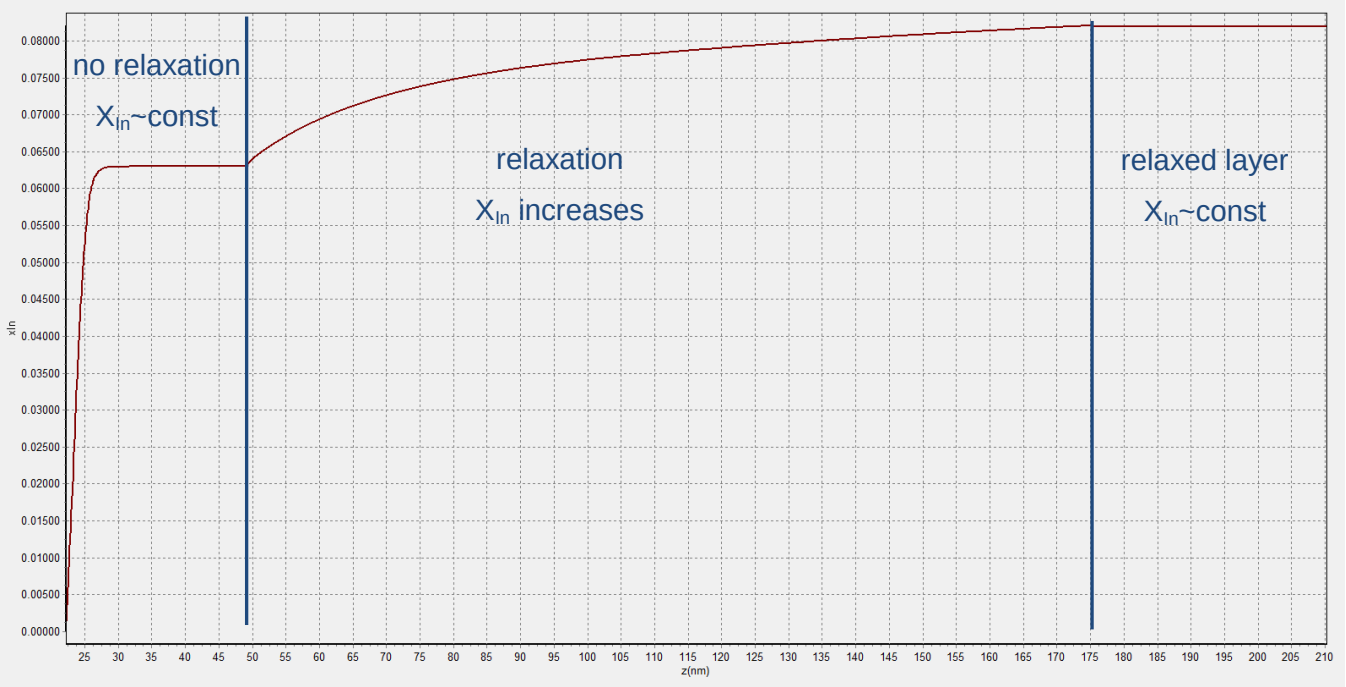

Fig. 9.9

9.6 Example 6: adding aluminum into barriers of MQW structures

One of the effective techniques to improve the emitting characteristics of the InGaN/GaN heterostructures is the introduction of tensile AlGaN layers into the GaN barriers, which compensate for the compressive strain in the InGaN MQWs (so called strain compensated mechanism). Using this technique, it becomes possible to increase the indium content in the QWs and to shift the peak wavelength in the green and even yellow/amber spectral area without degradation of the heterostructure quality and with higher emission intensity (Ref. [12]).The effect is associated, in particular, with the suppression of V-shaped dislocation HL nucleation that is related within our model to a lower energy release of the biaxial mismatch stress to produce the dislocation HL. The example illustrates how this effect is reproduced with STREEM-InGaN.

We use the growth conditions close to those given in Example 9.4 but with temperatures of 715 °C and 940 °C for growth of $In_{0.21}Ga_{0.79}N$ QWs and (Al)GaN barriers, respectively, as it is reported in [12]. Following this paper, we first consider the growth of tenfold $In_{0.21}Ga_{0.79}N$/GaN/GaN heterostructure with

the barrier thickness of ~17 nm (sample A). Then we consider three similar heterostructures where a layer of $Al_{0.2}Ga_{0.8}N$ of increasing thickness is introduced into the GaN barrier so that the total barrier thickness is kept approximately constant (samples A1, A2, A3). The growth recipes corresponding to samples A and A1 are presented in Fig. 9.10 (top and bottom, respectively). Recipes for samples A2 and A3 differ from that for sample A1 only by the durations of stages “AlGaN barrier” and “GaN barrier” (234 sec and 647 sec for A2 and 477 sec and 390 sec for A3).

A

Main Parameters | KineticData | Before Active Region | Active Region | After Active Region

Repeat Count	Stage Number	Name	Duration sec	Temperature C	Pressure Torr	N2 FlowRate slm	H2 FlowRate slm	NH3 FlowRate slm	TMIn FlowRate,µmol/r Bub.	TMIn FlowRate,µmol/r Given	TMGa FlowRate,µmol/r Bub.	TMGa FlowRate,µmol/r Given	TEGa FlowRate,µmol/r Bub.	TEGa FlowRate,µmol/r Given	TMAl FlowRate,µmol/m Bub.	TMAl FlowRate,µmol/m Given
10	1	QW	135	715	350	4	0	4	☐	2.3266	☐	6,0037	☐	0	☐	0
				715	350	4	0	4	☐	2.3266	☐	6,0037	☐	0	☐	0
	2	GaN cap	180	715	350	4	0	4	☐	0	☐	6,0037	☐	0	☐	0
				715	350	4	0	4	☐	0	☐	6,0037	☐	0	☐	0
	3	Ramping	100	715	350	4	0	4	☐	0	☐	0	☐	0	☐	0
				940	350	4	0	4	☐	0	☐	0	☐	0	☐	0
	4	GaN barrier	850	940	350	4	0	4	☐	0	☐	6,0037	☐	0	☐	0
				940	350	4	0	4	☐	0	☐	6,0037	☐	0	☐	0
	5	Ramping	100	940	350	4	0	4	☐	0	☐	0	☐	0	☐	0
				715	350	4	0	4	☐	0	☐	0	☐	0	☐	0

A1

Main Parameters | KineticData | Before Active Region | Active Region | After Active Region

Repeat Count	Stage Number	Name	Duration sec	Temperature C	Pressure Torr	N2 FlowRate slm	H2 FlowRate slm	NH3 FlowRate slm	TMIn FlowRate,µmol/r Bub.	TMIn FlowRate,µmol/r Given	TMGa FlowRate,µmol/r Bub.	TMGa FlowRate,µmol/r Given	TEGa FlowRate,µmol/r Bub.	TEGa FlowRate,µmol/r Given	TMAl FlowRate,µmol/m Bub.	TMAl FlowRate,µmol/m Given
10	1	QW	135	715	350	4	0	4	☐	2.3266	☐	6,0037	☐	0	☐	0
				715	350	4	0	4	☐	2.3266	☐	6,0037	☐	0	☐	0
	2	GaN cap	180	715	350	4	0	4	☐	0	☐	6,0037	☐	0	☐	0
				715	350	4	0	4	☐	0	☐	6,0037	☐	0	☐	0
	3	Ramping	100	715	350	4	0	4	☐	0	☐	0	☐	0	☐	0
				940	350	4	0	4	☐	0	☐	0	☐	0	☐	0
	4	AlGaN barrier	63	940	350	4	0	4	☐	0	☐	6,0037	☐	0	☐	1.37
				940	350	4	0	4	☐	0	☐	6,0037	☐	0	☐	1.37
	5	GaN barrier	870	940	350	4	0	4	☐	0	☐	6,0037	☐	0	☐	0
				940	350	4	0	4	☐	0	☐	6,0037	☐	0	☐	0
	6	Ramping	100	940	350	4	0	4	☐	0	☐	0	☐	0	☐	0
				715	350	4	0	4	☐	0	☐	0	☐	0	☐	0

Fig. 9.10

Calculated dependencies of the threading dislocation density at the growth surface on the coordinate of this surface for samples A, A1, A2, and A3 are presented in Fig. 9.11 (left vertical axes, brown curves). For better clarity, corresponding profiles of the AlN molar fraction in the heterostructure are also plotted here (right vertical axes, blue curves). It is seen from these results that the point of generation of dislocation HLs shifts to the higher thickness and the dislocation density reduces as the AlGaN layers appear and become thicker. For the thickest AlGaN layers (sample A3) the dislocation HLs are not produced at all. This finding qualitatively agrees with the experimental observation of the higher PL intensity at thicker AlGaN layers.

Note that the dislocation density for sample A3 looks constant in Fig. 9.11 due to the use of common scale of the left vertical axis for all cases. However, being plotted in the auto-scale, the dislocation density is seen to remain constant within the AlGaN layers only. In all the other regions it slightly decreases (Fig. 9.12). The effect is related to the annihilation of the sloped dislocations in the compressed regions of the structure that does not occur in the tensile AlGaN layers.

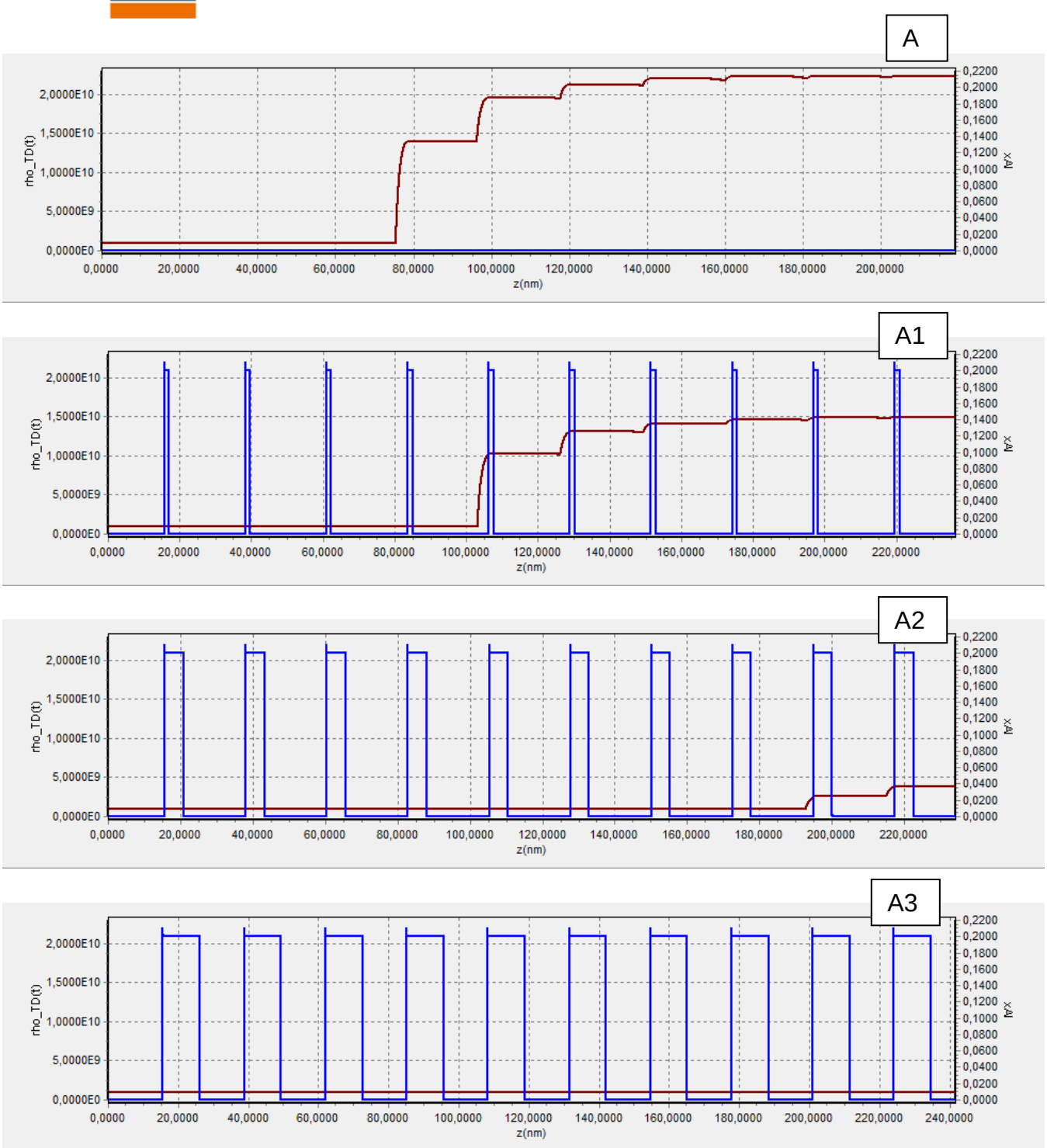

Fig. 9.11

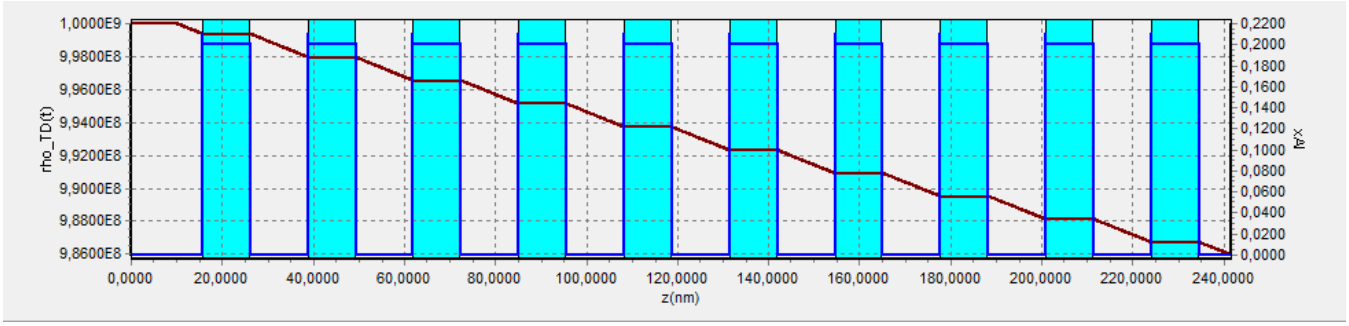

Fig. 9.12

9.7 Example 7: lattice-matched AlInN/GaN distributed Bragg reflectors

To illustrate capability of the STREEM-InGaN software, we have included an example of the software application to the modeling of the AlInN/GaN distributed Bragg reflectors. It is well known that high quality and long lifetime of such structures can be achieved using so called lattice-matched AlInN layers with ~18% In content. This composition provides the same lattice constants of AlInN and GaN and thus reduces generation of various defects in the structure – see Ref. [13].

The growth conditions in this example generally correspond to those in the above paper. In particular, the AlInN layers were grown under N_2 as the carrier gas at the temperature of 800 °C, pressure of 70 mbar, and NH_3 flow rate of 900 sccm. Then, for the growth of GaN layers, the carrier gas was changed to H_2, the temperature and the pressure were raised to 1115 °C and 200 mbar, respectively, and the NH_3 flow rate was increased to 2000 sccm. Thicknesses of the AlInN and GaN layers were chosen as 47 nm and 43 nm. The whole recipe is presented in Fig. 9.13.

Main Parameters | KineticData | Before Active Region | Active Region | After Active Region

Repeat Count	Stage Number	Name	Duration sec	Diffusion layer thickness,	Pressure mbar	N2 FlowRate slm	H2 FlowRate slm	NH3 FlowRate slm	TMIn FlowRate,sccm		TMGa FlowRate,sccm		TEGa FlowRate,sccm		TMAl FlowRate,sccm	
									Bub.	Given	Bub.	Given	Bub.	Given	Bub.	Given
	1	Inter_Buffer_AlInN1	1	1	7000	2.7	0	0.9	☐	0	☐	0.3	☐	0	☐	0
					7000	2.7	0	0.9	☐	0.06	☐	0	☐	0	☐	0.24
10	2	AlInN1	430	1	7000	2.7	0	0.9	☐	0.06	☐	0	☐	0	☐	0.24
					7000	2.7	0	0.9	☐	0.06	☐	0	☐	0	☐	0.24
	3	Inter_AlInN1_GaN1	1	1	7000	2.7	0	0.9	☐	0.06	☐	0	☐	0	☐	0.24
					7000	2.7	0	0.9	☐	0	☐	0.3	☐	0	☐	0
	4	Tramp_AlInN1_GaN1	60	1	7000	2.7	0	0.9	☐	0	☐	0.3	☐	0	☐	0
					7000	2.7	0	0.9	☐	0	☐	0.3	☐	0	☐	0
	5	H2N2change_AlInN1_GaN1	1	1	7000	2.7	0	0.9	☐	0	☐	0.3	☐	0	☐	0
					20000	0	6	2	☐	0	☐	0.3	☐	0	☐	0
	6	GaN1	205	1	20000	0	6	2	☐	0	☐	0.3	☐	0	☐	0
					20000	0	6	2	☐	0	☐	0.3	☐	0	☐	0
	7	H2N2change_GaN1_AlInN2	1	1	20000	0	6	2	☐	0	☐	0.3	☐	0	☐	0
					7000	2.7	0	2	☐	0	☐	0.3	☐	0	☐	0
	8	Tramp_GaN1_AlInN2	60	1	7000	2.7	0	0.9	☐	0	☐	0.3	☐	0	☐	0
					7000	2.7	0	0.9	☐	0	☐	0.3	☐	0	☐	0

Fig. 9.13

Calculated profiles of the InN, GaN, and AlN molar fractions in combination with the distribution of the threading dislocation density are presented in Fig. 9.14. The figure shows that the recipe provides the desired lattice-matched composition of the AlInN layers while the InN “tails” looks rather short in the

thick GaN layers. Correspondingly, the V-shaped dislocation HLs are not generated in this case and the dislocation density exhibits the same behavior as in case A3, Example 6 (annihilation in the compressed GaN regions and constant number in the tensile AlInN regions).

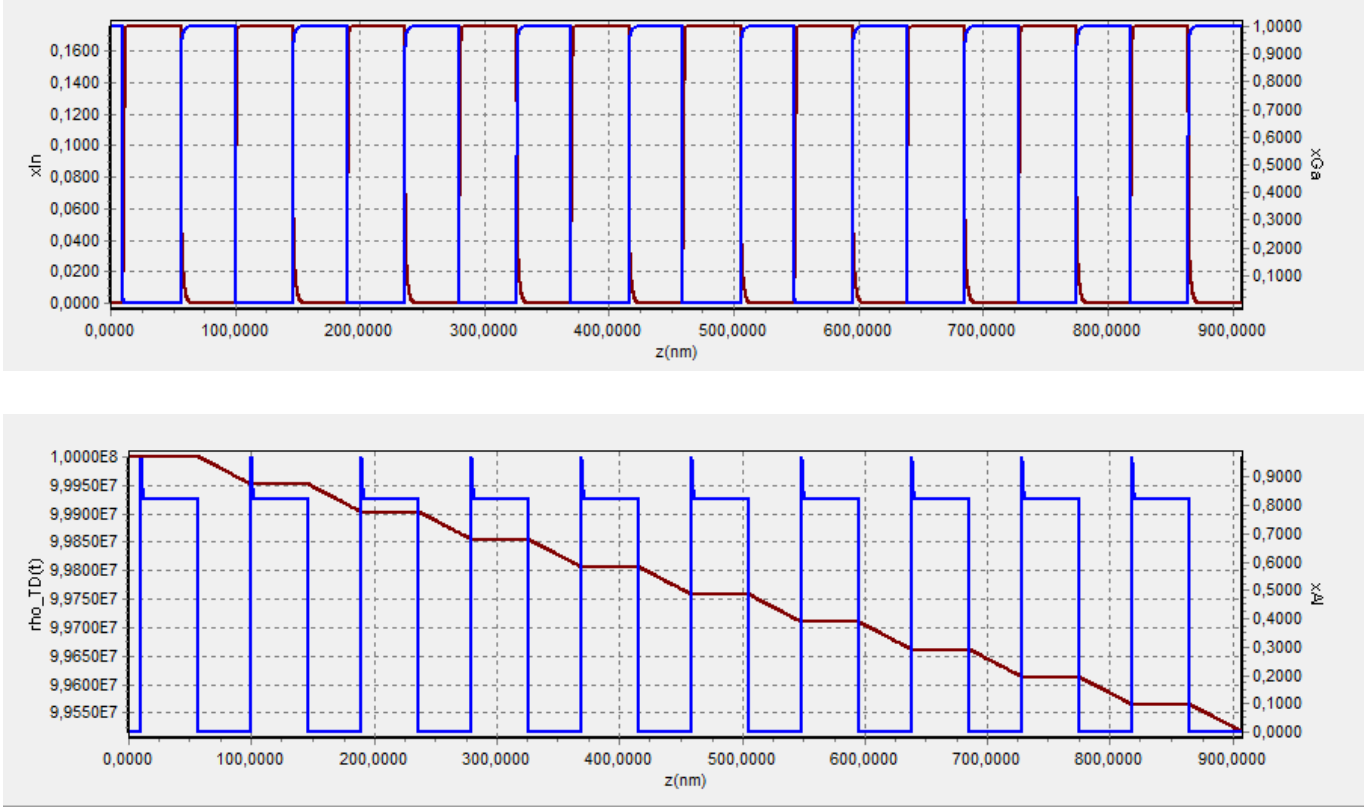

Fig. 9.14

10. References

[1] S.Yu. Karpov, R.A. Talalaev, I.Yu. Evstratov, and Yu.N. Makarov: “Indium segregation kinetics in MOVPE of InGaN-based heterostructures”, Phys. Stat. Sol. (A) 192 (2) (2002) 417.

[2] E.V. Yakovlev, A.S. Segal, K.A. Bulashevich, S.Yu. Karpov, and R.A. Talalaev: “Correlations Between Epitaxy Recipe, Characteristics, and Performance of Nitride Light Emitting Diode Structures”, Jpn. J. Appl. Phys 52 (2013) 08JB15.

[3] A. Segal, E. Yakovlev, S. Karpov, M. Korytov, N. Cherkashin, J. Bassen, H.-J. Lugauer, and H. Laux: “Atomic-scale composition profiles of MOCVD-grown InGaN/GaN quantum wells: modeling and characterization”, presented at IWN-2014, August 24-29, Wroclaw, Poland (2014).

[4] A.S. Jordan: “Activity coefficients for a regular multicomponent solution”, J. Electrochem. Soc. 119 (1972) 123.

[5] S.Yu. Karpov: “Suppression of phase separation in InGaN due to elastic strain”, MRS Internet J. Nitr. Semicond. Res. 3, 16 (1998).

[6] A.V. Lobanova, A.L. Kolesnikova, A.E. Romanov, S.Yu. Karpov, M. E. Rudinsky, and E. V. Yakovlev: “Mechanism of stress relaxation in (0001) InGaN/GaN via formation of V-shaped dislocation half-loops”, Appl. Phys. Lett. 103 (2013) 152106.

[7] A. Romanov, W. Pompe, G. Beltz, and J. Speck: “Modeling of threading dislocation density reduction in heteroepitaxial layers”, Phys. Stat. Sol. (b) 198 (1996) 599.

[8] O.Kayser, H.Heinecke, A.Brauers, H.Luth, P.Balk, Chemtronics, 3 (2) (1988) 90

[9] A.V. Sakharov, W.V. Lundin, E.E. Zavarin, M.A. Sinitsyn, A.E. Nikolaev, S.O. Usov, V.S. Sizov, G.A. Mikhailovsky, N.A. Cherkashin, M. Hytch, F Hue, E.V. Yakovlev, A.V. Lobanova and A.F. Tsatsulnikov: “Effect of strain relaxation on active-region formation in InGaN/(Al)GaN heterostructures for green LEDs”, Semiconductors, 43 (6) (2009) 812.

[10] A.V. Lobanova, A.L. Kolesnikova, A.E. Romanov, S.Yu. Karpov, M.E. Rudinsky, E.V. Yakovlev, Yu.A. Shpolyanskiy: “New Mechanism of Stress Relaxation in (0001) InGaN-Based Heterostructures”, presented at ICNS-10, August 25-30, Washington, USA (2013).

[11] D. M. Van Den Broeck, D. Bharrat, A. M. Hosalli, N. A. El-Masry, and S. M. Bedair: “Strain-balanced InGaN/GaN multiple quantum wells”, Appl. Phys. Lett. 105 (2014) 031107.

[12] K. Lekhal, B. Damilano, H.T. Ngo, D. Rosales, P. De Mierry, S. Hussain, P. Vennegues, and B. Gil: “Strain-compensated (Ga,In)N/(Al,Ga)N/GaN multiple quantum wells for improved yellow/amber light emission”, Appl. Phys. Lett. 106 (2015) 142101.

[13] C. Berger, A. Dadgar, J .Blasing, A. Lesnik, P. Veit, G. Schmidt, T. Hempel, J. Christen, A. Krost, and A. Strittmatter: ”Growth of AlInN/GaN distributed Bragg reflectors with improved interface quality”, J.

Cryst. Growth 414 (2015) 105.